Probing the structure and function of cystic fibrosis transmembrane conductance regulator using chemical modification

PhD dissertation

Zhi-Ren Zhang, MD

Semmelweis University
Doctoral School of Basic Medicine

Mentor: **Nael A. McCarty, Ph.D.,** Associate Professor and Senior CF Scientist, Division of Pulmonology, Allergy/Immunology, Cystic Fibrosis, and Sleep Department of Pediatrics, Emory, USA

Tutor: Prof. Dr **László Rosivall, MD, Ph.D., DSc**, Director, Renal Research and Training Center, Institute of Pathophysiology, Semmelweis University

Program Leader: **László Rosivall, MD, PhD, DSc**
Official Academic Reviewers: **László Csanády, MD, PhD**
President of the Examining Committee: **Emil Monos, MD, PhD, DSc**
Examining Committee Members:
László Csanády, MD, PhD
Norbert Hajós, MD, PhD

2008, Budapest

Table of Contents

List of abbreviations

CFTR, cystic fibrosis transmembrane conductance regulator;

PKA, protein kinase A

cRNA, clonal ribonucleic acid

$MTSET^+$, [2-(trimethylammonium)ethyl] methanethiosulfonate;

$MTSES^-$, 2-sulfonatoethyl methanethiosulfonate; 2-ME, 2-mercaptoethanol

DTT, dithiothreitol;

HEPES, 4-(2-hydroxyethyl)piperazine-1-ethanesulfonic acid

MES, 2-morpholinoethanesulfonic acid

TES, N-[tris(hydroxymethyl)methyl]-2-aminoethanesulfonic acid

NMDG, N-methyl-D-glucamine

AMP-PNP, 5'-adenylyl-β, γ-imidodiphosphate.

TEVC, two-electrode voltage clamp

1. Introduction:

1.1. An overview

The cystic fibrosis transmembrane conductance regulator (CFTR) is a chloride channel and the gene defective in cystic fibrosis (CF) encodes CFTR [1], a member of the ATP-Binding Cassette (ABC) Transporter superfamily [2] which includes other several proteins of clinical relevance, such as p-glycoprotein. CFTR is 1480 amino acids long with a mass of approximately 170 kDa. The predicted secondary structure of CFTR is novel to ion channels. It consists of five functional domains: two hydrophobic membrane-spanning domains (MSD1, MSD2; Fig. 1), each including 6 transmembrane (TM) helices; two hydrophilic stretches that form nucleotide-binding domains (NBD1, NBD2); and a unique regulatory (R) domain which carries multiple protein kinase A (PKA) consensus sites. Members of the ABC superfamily catalyze the ATP-dependent membrane transport of a wide variety of substrates ranging from small inorganic ions and metabolites to large hydrophobic drugs and polypeptides. However, CFTR is unique in this group in that it functions as an ion channel. Conversely, no other pore-forming ion channel subunit exhibits the domain architecture characteristic of an ABC transporter.

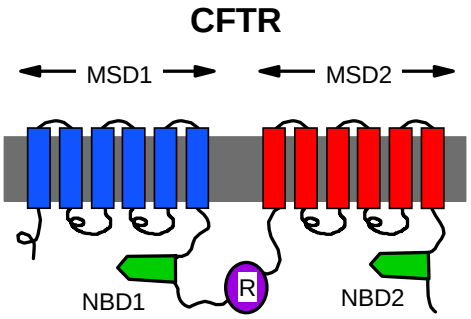

Fig. 1. The two-dimensional model shows the domain architecture of CFTR.

CFTR is a multifunctional protein and is principally expressed in epithelial tissues, where it plays a crucial role in regulating the quantity and composition of epithelial secretions. However, an examination of the physiology of the individual epithelia where CFTR is expressed reveals tissue-specific differences in CFTR function. A variety of factors contribute to this diversity including tissue architecture, interacting

proteins and the function of CFTR both as a chloride channel and as a regulator of ion channels and transporters [3; 4]. CFTR regulates the activity of several other types of ion channel [5; 6; 7], including ORCC chloride channels [6], ENaC sodium channels [8], ROMK2 potassium channels [9] and Kir6.1 potassium channels [10], although the mechanisms by which it does so are not clear [11]. Recent work suggests that CFTR plays a role in receptor-mediated endocytosis in the proximal tubule and its absence causes low molecular weight proteinuria [12]. CFTR also plays an important role in cardiac electrophysiology and pathophysiology; for instance, activation of sarcolemmal CFTR Cl^- channels can significantly alter the resting membrane potential and affect the duration of the action potential [13]. CF causes widespread involvement of the cardiovascular system. Aside from the heart, unusual aberrations have been observed in the bronchial arteries, the aorta, and the systemic capillaries [14]. In infant CF patients usually 24 months of age or less, severe cardiac necrosis and scarring fibrosis often causes complications of CF leading to a sudden, unexpected fatal cardiac arrest [15].

1.2. Why it is important to study the structure and function of the CFTR channel?

CF is a fatal disease affecting the lungs and diversity systems including intestine, pancreatic, sweat ducts and heart by impairment of the CFTR chloride channel. CF affects approximately 30,000 patients in America and many more worldwide. The majority of CF patients are linked to the deletion of an amino acid phenylalanine 508 (ΔF508). ΔF508 is located in the NBD1 and it is sufficient to impair the trafficking of CFTR to the plasma membrane and therefore to impair its function. Despite ΔF508, more than 1400 mutations have been identified so far as CF associated [www.genet.sickkids.on.ca; 16]. CFTR is also a key element in other two diseases of note: polycystic kidney disease (PKD) and secretory diarrhea including cholera. Therefore, understanding the structure and function of CFTR chloride channel is important and clinically relevant. For example, the development of pharmacological modulators for CF requires a better understanding of the function of the normal channel; also activation of CFTR in cholera leads to a life-threatening dehydration and activation of CFTR in PKD results in fluid-filled cysts. In these cases, understanding the structure

of the pore may leads to the design of clinically useful inhibitors to cure the rampant secretion associated with these conditions. Understanding the structure and function of CFTR is also important because CFTR is a member of the ABC transporter superfamily; the conformational changes experienced by the pore of CFTR may reflect the ontogeny of this channel as a member of the ABC superfamily. Compared to transporters, we can study the channel with extremely high resolution using the patch-clamp technique, we may be able to extrapolate the observations in CFTR to deciphering how the substrate binding pocket of ABC transporters changes structure during the pump cycle.

1.3. Regulation of CFTR channel gating by intracellular ATP

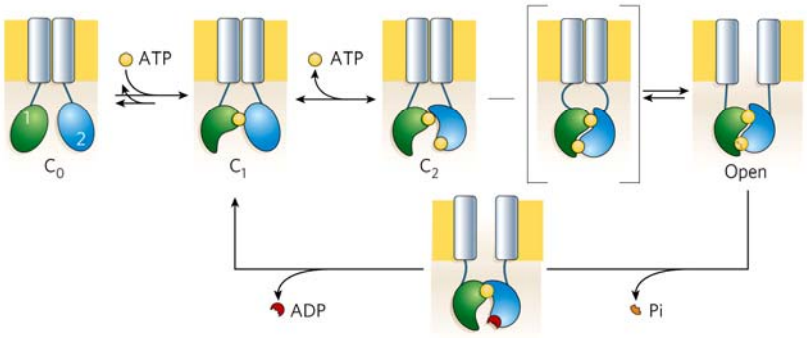

***Fig. 2.* A simple scheme of ATP-dependent gating cycle of phosphorylated CFTR channel.** The yellow filled circles represent ATP molecules. NBD1 and NBD2 depicted as green and blue, respectively. Transmembrane pore indicated by the grey rectangles. **Adopted from Gadsby *et al.*, 2006. *Nature*.**

The first piece evidence for CFTR being an ATP-gated ion channel was revealed by Anderson and coworkers [17]. They expressed human CFTR either stably in NIH-3T3 cells, or transiently in Hela cells and demonstrated that CFTR activation requires phosphorylation by PKA using inside-out patches, and that hydrolysable nucleoside triphosphates, such as ATP, GTP, ITP, CTP and UTP, are needed to open the phosphorylated channels. Nagel and coworkers confirmed these results by examining the endogenous CFTR in cardiac myocytes isolated from guinea pig [18]. These early

efforts nicely provide hints on later studies of gating mechanism of CFTR, i.e. functional role of R domain and NBDs.

Although it is well accepted that phosphorylation of R-domain is required for CFTR activation; however, the question as to how the R-domain regulates the channels is still controversial. It has shown that truncated R-domain results in channels that conduct chloride in the absence of cAMP stimulation [19]. In excised inside-out patches, this partially R-domain deleted CFTR can be opened by ATP without PKA-dependent phosphorylation. This phosphorylation-independent activity was confirmed by later studies in which the R-domain completely deleted [20; 21]. These results together suggest that the R-domain of CFTR serves, at least, as an inhibitor for channel gating by ATP. However, how phosphorylation of individual serine residues in the R-domain controls CFTR function remains poorly understood. Nevertheless, CFTR channel gating is dependent upon phosphorylation of its R-domain, and upon binding and hydrolysis of ATP at the NBDs.

A few current ATP-dependent gating models of CFTR have been proposed by several groups; these groups attempt to identify the mechanisms of action of NBDs and the sequence of events related to opening and closing the channel pore [22-24]. A recent model of CFTR gating proposed by Dr. Gadsby and co-workers describes ATP binding as a switch that controls dimerization of the two NBDs, where binding of ATP leads to dimerization of the two NBDs, which is linked to channel opening, while hydrolysis of ATP causes disassociation of the dimers and subsequent channel closure [25; 26] (see Fig. 2) In this model, one ATP-binding site is comprised of the Walker A and Walker B sequences of one NBD coupled with the LSGGQ "ABC signature sequence" contributed by the other NBD. This ATP-induced dimerization concept is consistent with the crystal structure of NBDs published to date [27-31]. In most ATPases, the NBD domains are identical; however, CFTR's NBDs exhibit structural divergence (only 27% identity) [25; 32]. Consistent with this model, the Bear lab showed that purified NBD1 and NBD2, by themselves, sustained only poor ATP hydrolysis rates [32]. When two NBDs combined, the ATPase activity was enhanced 2-3 fold. Hence, dimerization of the two NBDs is required in order to achieve optimal ATPase activity. Furthermore,

using photolabeling experiments, Basso *et al*. [33] suggested that the nucleotide interactions (binding and hydrolysis) that time the opening and closing of CFTR occur predominantly at NBD2, while ATP remains tightly bound at NBD1 for longer periods. The rate-limiting step for channel opening, therefore, is binding of ATP at NBD2, and hydrolysis of that bound nucleotide leads to rapid channel closure. When hydrolysis at NBD2 is slowed by mutation or in the presence of poorly-hydrolyzable nucleotides, channels close by a 100-fold slower pathway that involves dissociation of the unhydrolyzed nucleotide [34].

Despite the great progress has made thus far by several groups, there are still questions remaining with regard to the complex gating process of CFTR. For instance, the role of ATP binding at NBD1 in triggering channel to open remains controversial [35-40]. One possible explanation for the controversial results obtained by different investigator could be that they use different expression systems and CFTR gating is subjective to modulations by differential phosphorylation of the R-domain. There are several questions to be answered with regard to the dimerization process as well. For instance, how does ATP binding at the Walker A and B motifs catalyze the formation of the dimmer? How is the signature sequence recruited to contact the bound ATP? Interestingly, Dr. Hwang has questioned whether the dimerization of the NBDs is the only mechanism for CFTR channel to open, based upon their observation that CFTR channels open even in the absence of ATP albeit with a very low open probability [21; 41]. A study carried out by Wang and coworkers describes that activity of CFTR channels can be enhanced when NBD2 completely deleted [42].

1.4. Conduction property of CFTR

Human CFTR chloride exhibits a low single-channel conductance, typically 8-10 pS at room temperature in the presence of 150 mM symmetrical chloride. Wild-type (WT) CFTR currents exhibits no voltage- or time-dependence, over steps ranging from 1 msec to several seconds to the potentials between -100 mV to +80 mV. Like most other anion channels do, CFTR does not discriminate perfectly between anions and

cations: these channels typically show only a 10-fold preference for chloride over sodium [43; 44].

It has been suggested that CFTR is a multi-ion pore capable of holding multiple anions simultaneously. This feature of the CFTR pore could be a key determinant of the channel's conduction properties because repulsive interactions between anions inside the pore ensure rapid anion permeation [45]. As reported by Liu and coworkers, anion flow through the CFTR pore is determined by anion permeability and the ease with which anions enter the CFTR pore, and the ability of anion binding (the tightness of the interaction between anions and the CFTR pore). It has been demonstrated that the anion permeability sequence of CFTR follows a lyotropic sequence [46]. This suggests that anion permeation is determined by the hydration energy of anions with large, weakly hydrated anions being most permeant [47]. Hence, anion binding exhibits a lyotropic sequence with large anions binding tighter to the CFTR pore. This tight binding of large anions (e.g. $Au(CN)_2$) within the CFTR pore explains why these anions blocks chloride anion permeation avidly [48]. A novel feature of the CFTR pore is that selectivity is "dynamic" (refer to Section 1.10). This may suggest that there is link between the permeation properties and gating events of CFTR, as it appears to be the case in several other channels. For instance, CFTR allows permeation of large organic anions when present at the intracellular but not the extracellular side of an excised patch; this asymmetry is dependent upon ATP hydrolysis [49-52].

Over ~2 decades since the cloning of the human CFTR gene, progress has been made in defining portions of the protein comprising pore-lining domains and residues within those domains that play important role in establishing the biophysical character of open CFTR channels [53]. Welsh and coworkers used chimera studies to show that differences between *Xenopus laevis* and human CFTR were governed by MSD1 [54]. In this study, they found that there are only very minor differences between human and *Xenopus laevis* versions of TM11 and TM12. The results of this study may suggest that all the important residues in MSD2 are the same in these two species. Also, the limited assay used in this study may be insufficient for showing other functional differences that may be determined by MSD2. The results from studying of regional deletion

mutants have also suggested that the sequences in TM1-TM6 might be sufficient for formation of the pore, but it may require dimerization of the half-channel protein to function [11; 55]. Other investigators have found that the N terminus of CFTR, including TM1-TM4, could be deleted without loss of function [56]. A splice variant similar to this is expressed in the kidney [57]. Hence, it has been proposed that TM5-TM6, together with all of MSD2 and intracellular domains, may be the minimum component for CFTR channel to function. Other studies have shown that channels may be constructed from only C-terminal half of CFTR, although these channels were not selective between Cl^- and I^- [58]. Mutagenesis studies also suggested that the portions of CFTR that function in Cl^- conduction were separate from the portions contributing to regulation of ORCC [11].

In the present time, we do not know how many TM domains contribute the formation of the CFTR conduction pathway. There has been no unequivocal evidence that CFTR pores require two or more subunits, except in cases where truncated mutations were expressed. Data obtained from expression of recombinant CFTR in a variety of cell models suggest that CFTR may exit in monomeric form [59]. Concatamerized constructs expressed in HEK-293 cells show that cytoplasmic regulatory domains from two CFTRs can interact, although it was not clear that both constructs contributed to only one pore [60; 61]. Freeze-fracture studies also suggested that heterologously expressed CFTR may be found in the membrane as dimers [62], although these methods cannot distinguish between models with one or two pores. Dimerization of HisP, the ATP-binding subunit of the histidine permease, appears to be required for function [63; 64]. However, because HisP is equivalent to only one of the NBDs of CFTR, this information is consistent with interaction between the two NBDs of CFTR, not between two CFTR monomers. It appears that the possibility exists that the functional CFTR channel is constructed from a dimer of CFTR peptides [65]. A dual-pore model has even been suggested by computer modeling [66], although this study was performed without much regard to the large body of physiological data available.

Anderson and coworkers assessed the first structure/function studies in CFTR, in which they tested charge-reversal mutations in TM1, TM6 and TM10 [44]; mutations at two of the four residues studied resulted in modest changes in halide selectivity. Based upon their observations, these authors concluded that TM1 and TM6 contributed to the pore. Synthetic peptides with sequences of TM2 and TM6, but not other TMs in MSD1, produced Cl^- selectivity channels when incorporated into lipid bilayers [67; 68]. Akabas and coworkers used cysteine-scanning mutagenesis to study TM1; they identified that a surface of the TM1 helix appears to line the pore and later they extended that work to TM6 and TM3 [69; 70], although they did include neither the appropriate control experiments nor single-channel recordings. Therefore, their results based on cysteine-scanning assays remain uncertainty (refer to Section *covalent labeling probes the structure and function of CFTR*).

Recently, a low resolution crystal structure of CFTR was obtained [71], which showed membrane-spanning regions lining a central pore, the pathway through which chloride ions cross the membrane. Unfortunately, the identity of the TM regions forming the pore, or even the number of TMs that line the pore, cannot be identified in this structure. Among the TMs of CFTR, TM6 has been drawing the most attention of investigators and has been identified by a number of laboratories as a potential element of the CFTR pore [7; 44; 47; 72-75]. McCarty group has previously systematically explored the potential role of regions of TM6 in anion permeation and binding by comparison permeability ratios and conductance ratios seen in the presence of substitute anions in the solution bathing *Xenopus* oocytes for a series of alanine mutants extending position 335 to 341 [7]. The observations in this study are consistent with the findings of Linsdell *et al.* [47] and suggest that the possibility that CFTR pore may begin to narrow in a region near T338. Glutamic acid substitution at 338 and 341 disrupted anion binding as if these residues may lie in the vicinity of, or in some way contribute to, the structure of an anion binding site [7]. One of the reasons why TM6 has been receiving such extensive attention is that: TM6 is the helix and includes a greater number of charged amino acids than any other TMs. McDonough *et al.* recognized homology between TM6 sequence and the sequence of the pore-lining domain of the ligand-gated chloride channels formed by the $GABA_AR$ and GlyR [76]. Some early studies seemed

to implicate arginines in binding of either chloride or thiocyanate by proteins [43]. Arginine 347 had been proposed to comprise part of such a binding site in CFTR because the anomalous mole fraction effect seen with symmetrical SCN^- was absent in R347 mutants [77]. In contrast, Cotton and Welsh suggested that this residue might function to stabilize CFTR core structure by forming a salt-bridge with D924 in TM8 [78]. However, Smith *et al*. reported that a cysteine substituted for R347 was not accessible to polar thiol reagents and they concluded that the nature and location of an anion coordination site in CFTR remains largely a matter of speculation at present [79].

It is unlikely that the pore of this putatively monomeirc channel protein is constructed from a single TM helix; other domains must also contribute amino acids to the pore. Dawson and coworkers have suggested that TM5 may contribute to the pore on the basis of their findings that mutations at G314 and V317 in this domain alter conduction properties [74; 79]. McCarty and coworkers suggested that TM11 and TM12 also contribute to the pore based upon the data obtained from selectivity studies and from an analysis of the effects of mutations in these domains upon interactions with open-channel blockers (refer to next Section).

1.5. CFTR channel blockers provide the information of pore structure

Channel blockers have been used to define the structure and function of ion channels [80]. Pore-blocking drugs are used as probes of the pore structure, by assessing the effects of mutagenesis upon blocking behavior [81; 82]. Although a wide variety of organic compounds have been shown to inhibit CFTR, only a few have been shown to inhibit CFTR via an open-channel block mechanism. Two families of compounds (arylaminobenzoates and sulfonylureas) have been extensively studied as blockers of CFTR pore. The arylaminobenzoates, whose parent compound is diphenylamine-2-carboxylate (DPC), block CFTR via a simple bimolecular interaction with a site accessible from the intracellular side of the CFTR pore [83-85]. DPC and its congener flufenamic acid (FFA) were shown by McCarty and coworkers to block single CFTR channels with simple kinetics, *i. e.,* application of drug to the cytoplasmic media

introduced a single class of closed states into recordings from excised patches [86]. Subsequent studies indicated that a dose-efficacy relationship for DPC block of CFTR macroscopic currents was fit best with a Hill-coefficient near unity [84]. These observations suggest that DPC interacts with a single site of CFTR. Blockade of both macroscopic currents and single-channel currents are sensitive to membrane voltage and to the concentration of permeation anion, consistent with the notion that DPC blocks CFTR by entering the pore [76]. DPC and NPPB (5-nitro-2-(3-phenylpropylamino)-benzoate) block CFTR by the classical open-channel block mechanism as evidenced by a drug-induced increase in burst duration [84]. The lengthening of the burst duration can be interpreted as an influence of the blocker on the conformational change required for channel closing. Burst durations are increased in direct proportion to the frequency and duration of blocking events. DPC and NPPB exhibit identical voltage-dependence of block of macroscopic current, suggesting that the two compounds bind at approximately the same position in the pore, accessed by traversing approximately ~40% of the voltage field across the membrane, as measured from the cytoplasmic side [84].

McCarty and coworkers attempted to identify amino acids which, when mutated, altered the interaction of arylaminobenzoate blockers with the pore. Several mutations were identified in TM6 and TM12 that affected affinity and/or voltage dependence of blockade by DPC [76], whereas several other mutations were found that affected neither affinity nor voltage dependence. Both the affinity and voltage-dependence of block were altered dramatically by mutation S341A in TM6. Mutations in TM12 also altered block by DPC, as did one mutation in TM11 [87]. Block of whole-cell currents by NPPB was impacted by the S341A and T1134F mutations in a manner somewhat different from the effects of these mutations on block by DPC [84]. These data indicate that although NPPB and DPC bind at similar positions, their interactions with the pore interior are not identical.

The sulfonylureas are hypoglycemic agents that interact with the sulfonylurea receptor (SUR, another member of the ABC Transporter superfamily) and are used clinically to control the release of insulin from pancreatic beta cells. The most potent sulfonylurea for this purpose is glibenclamide [88]. Glibenclamide and its congener,

tolbutamide, blocked CFTR whole-cell currents in mammalian cell lines with no apparent voltage-dependence. Subsequent studies attempted to identify the mechanism of interaction by utilizing excised inside-out patches to show that glibenclamide binds to the cytoplasmic side of CFTR and reduces the P_O in a voltage- and concentration-dependent manner [89; 90].

Our previous studies of the microscopic kinetics of block of single WT-CFTR channels by glibenclamide under steady-state conditions described multiple classes of interactions between drug and channel that differed in concentration-, voltage-, and pH-dependence, which may reflect interactions with different sites [91]. Some interactions were characterized by rapid kinetics, some intermediate, and some slow, representing transitions between the open state and three glibenclamide-induced blocked states that we termed C1, C2, and C3, respectively (Fig. 3). State C1 is characterized by the fastest forward and reverse rates, while state C3 is characterized by the slowest forward and reverse rates. The kinetics of glibenclamide's interactions with the fast and intermediate kinetic states (C1 and C2) are on the same order as the kinetics of interaction with DPC and NPPB [76; 84; 86]. Block of CFTR macroscopic currents by DPC or NPPB is time-independent, reflecting rapid interactions with a single class of drug-binding sites [84]. However, the disparate kinetics of interaction between glibenclamide and its multiple apparent binding sites predict that block of macroscopic currents by this drug may be complex: the slow kinetics of glibenclamide's interaction with the C3 state suggest that block of CFTR whole-cell and macroscopic currents by this drug should exhibit time-dependence. Subsequently, we compared the kinetics of whole-cell currents from oocytes expressing wildtype (WT)-CFTR in the presence of DPC or NPPB, as simple pore blockers, with the kinetics of such currents in the presence of glibenclamide. Secondly, we showed that such kinetic studies are greatly facilitated by using the excised, inside-out macropatch configuration, which eliminates several difficulties associated with analysis of whole-cell currents. We then asked whether the voltage-dependence and concentration-dependence of the kinetics of blockade of macroscopic currents were consistent with the microscopic kinetics of interaction with each site identified in single-channel experiments. The results confirm the kinetic model derived from single-channel studies in WT-CFTR and suggest new

quantitative approaches for determining the effects of site-directed mutations at the (presumably separate) glibenclamide-binding sites in the channel pore [92] (Fig. 3).

Zhou and coworkers studied the block of CFTR using detached patches and a CFTR variant, K1250A-CFTR, characterized by long open times. The binding characteristics of two organic blockers, glibenclamide and isethionate, particularly, the observation that they block only from the intracellular side of the pore, supports that hypothesis that the pore has a wide internal vestibule [93]. It appears that the most important generalization emerging from blocker studies is that molecules like DPC, glibenclamide, DIDS and gluconate reach their binding sites from the cytoplasmic side [49; 94]. The size of these compounds is large when compared to permeant anions, suggesting that the pore may feature a relatively large cytoplasmic vestibule, comparable to that of the K^+ channel where TEA derivatives bind [95-98]. This basic organizational plan is seen in the crystal structure of the CFTR homologue, MsbA that shows a large cytoplasmic opening formed by the transmembrane domains [99].

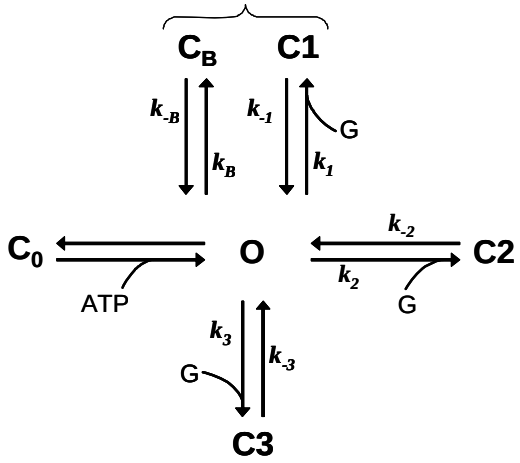

Fig. 3. **Kinetic model for block of WT-CFTR channels by glibenclamide (G), derived from single-channel recordings** (Zhang *et al.*, 2004). Phosphorylated channels open in an ATP-dependent manner from state C_0 to state O. From there, channels may be blocked with rapid kinetics by the background blocker (buffer, such as TES), leading to the C_B state, or by interactions with G, and leading to the C1 state. The C_B and C1 states are kinetically indistinguishable at a given G concentration as they are both characterized by blocked states < 1 ms in duration. G also interacts with two other sites with intermediate and slow kinetics leading to the C2 and C3 states, respectively

Recently, Verkman and coworkers discovered glycine hydrazide pore-occluding CFTR inhibitors [100]. These authors screened a collection of 100,000 diverse small molecules and revealed four novel chemical classes of CFTR inhibitors with much

lower K_i (in a range of <10 μM) compared to DPC, NPPB and glibenclamide. These compounds exhibit a novel inhibition mechanism involving occlusion near the external pore entrance. As discussed above, although use of these blockers has allowed us to gain insight into understanding the structure and function of CFTR; however, the most of these compounds block CFTR channels with low affinity and relatively poor specificity. It is exciting that McCarty's group has successfully identified a 3.7 kDa peptide inhibitor, which inhibits CFTR with very high affinity and specificity (refer to next section).

1.6. A newly discovered single peptide toxin, GaTx1, inhibits CFTR

Peptide toxins have proven to be among the most potent and selective antagonist available for voltage-gated channels permeable to K^+, Na^+ and Ca^{2+}, and have been very useful tools for detailed structural analysis of these proteins [101; 102]. These peptide toxins have provided detailed information about the arrangement of channel domains, about the interactions of the gating machinery with the pore [103]. On the other hand, peptide toxin gating modifiers also are useful tools to detect the gating mechanisms of ion channels. It also has been reported that peptide toxins have high potential as lead compounds for the development of therapeutics targeting pain, diabetes, multiple sclerosis, cardiovascular diseases and cancer [104]. To this end, McCarty group attempted to isolate a single peptide toxin from the scorpion *Leiurus quinquestriatus hebraeus* (Lqh). They previously reported that fractionated venom form Lqh inhibits CFTR in a voltage-independent manner by binding to the channel in a closed state when applied to its cytoplasmic surface [1075 106]. Most recently, these authors successfully utilized a bioassay-guided fractionation of scorpion venom to isolate a novel 3.7 kDa peptide toxin, GaTx1, which is a potent inhibitor of CFTR. GaTx1 is the first peptide toxin identified which inhibits a chloride channel of known molecular identity. It appears that GaTx1 inhibits CFTR in a state-dependent manner with a very high affinity and specificity, having a K_D in a range of 40-85 nM dependents upon the concentration of ATP used [107]. This finding may shed a light on defining both the permeation properties and the gating mechanisms of CFTR, as well as on defining the relationship

between changes in the pore conformation and ATP-dependent gating events at the NBDs.

1.7. A three-dimensional (3-D) model of the CFTR chloride channel Pore

Although TM6 has been extensively studied by many investigators and these studies have identified the critical role of TM6 in determining the permeation

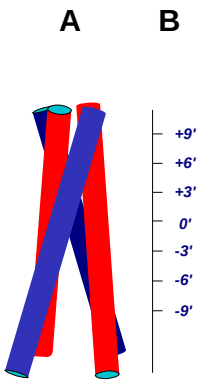

Fig. 4. **3-D fantasy model of the pore proposed by McCarty. (A)** Proposed orientation of four α-helices, TMs 5, 6, 11, and 12. The TM domains cross each other at a distance from the extracellular end (at top). We envision TM6 and 12 lying across the pore from each other (red pair or blue pair), and TM5 and 11 forming the other pair. **(B)** Vertical scale indicating the numbering system proposed for residues in these TM domains. For instance, S341 lies at position 0′, and T1134 lies at position +7′. The region of highest discrimination between anions would be comprised of amino acids between 0′ and +3′. **Adopted from McCarty, 2000.** ***The J of Experimental Biol.***

properties of CFTR; however, it is unlikely that a single α-helix is sufficient to form the pore because this one-dimensional view is very limited in its ability to describe the environment within the pore and cannot account for all the experimental data. The anions that permeate the pore and the drugs that block it are three-dimensional molecules and will probably interact with portions of the pore contributed by multiple TM domains. Therefore, it is important to consider the structure of the pore in three dimensions, taking into account the contributions made by amino acid residues in TM domains other than TM6 [83]. McCarty [83] proposed that the pore of CFTR is lined by residues contributed by TM domains 5, 6, 11 and 12 based upon the large scale systemic analysis of ion selectivity pattern between WT-CFTR and mutants-CFTR, and based on the effects of mutagenesis on blocking behaviors of open channel blockers. It is unfortunate that there is no high resolution crystal structure of CFTR available at the moment; a three-dimensional model of the CFTR pore proposed by McCarty may provide insight into the understanding the structure and function of CFTR (Fig. 4).

Most recently, Serohijos and coworkers constructed a 3-D structure of CFTR by molecular modeling and this 3-D model reveals important aspects of the interfaces between the BNDs and MSDs of CFTR. The most critical contact in conformational maturation during biosynthesis, which is precluded by the ΔF508 mutation, is between a site containing that residue on the surface the N-terminal NBD and a cytoplasmic loop in the C-terminal MSD [108]. This finding is consistent with and also helps to explain previous observations that CFTR membrane domains are disrupted by the ΔF508 mutation [108; 110]. They have identified the site of this interaction, dependent on the phenylalanine aromatic side chain. It appears to participate in an aromatic cluster with residues from cytoplasmic loop4 (CL4), which may contribute to the stability of this vital tertiary interaction as in other proteins [111; 112]. Studies by Serohijos [108] provide precise information on what has to be restored or mimicked to counteract the defect caused by the ΔF508 mutation. Further more, their findings also provide some insight into the role of this interface in the regulation of the CFTR channel. The formation of covalent cross-links between cysteines on either side of this interface arrests channel gating. This applies to both the Phe-508-contaning NBD1/CL4 interface and the counterpart between NBD2 and cytoplasmic loop2.

1.8. Covalent labeling probes the structure and function of CFTR

Since the "cysteine scanning" approach was pioneered by Karlin [113], this method has been used widely in many types of ion channels and the results from such studies have been providing insights into defining the structure and function of these proteins [114-123]. It was first applied to CFTR by Akabas [69; 70; 124-127]. The studies by Akabas and coworkers provided limited information with regards to the structure and function of the CFTR channel. There are some concerns regarding how they carried out the experiments, as well as interpretation of their data as follows: 1) in most of these studies, the action of the sulfhydryl-modifying (SH) reagents on single channels was not verified, although the authors recognized the need for such studies that would distinguish between effects on conductance and changes in gating; 2) the SH-

modifying reagents needed many minutes to take effect and true modification rates were not measured; 3) there was lack of appropriate control experiments which could ensure that the results obtained could be attributed to the single engineered cysteine; 4) membrane-permeant forms of SH-modifying reagents were used which could modify any of the endogenous cytoplasmic cysteines when applied from extracellular surface of membrane; and 6) the mechanism of action was not defined. Effects of SH-modifying reagents could be attributed to an endogenous cysteine(s) becoming available for modification due to conformational changes in pore structure, which could be caused by an allosteric effect of mutagenesis, as was seen for R352A-CFTR [79]. This exemplifies the need for a control at each position, so that sensitivity to SH-modifying reagents can be attributed to a known site. Therefore, one should always study both the cysteine substitution at a given position and the alanine at the same site. Without such a control, results could be misinterpreted as due to the X-to-Cys mutation, rather than an endogenous cysteine made accessible by an allosteric change in pore structure affected by substitution at position X. For mutants in which SH-reagents affected CFTR current, one should also ask whether the effects can be reversed by reducing agents DTT or 2-ME. If the impact of SH-reagent is reversible by washout using a solution without reducing agents, this indicates a non-covalent interaction.

In contrast, Dawson and McCarty [79; 128-130] groups conducted experiments on engineered cysteine residues using SH-modifying reagents with caution, analyzing the mechanism of modification, and the results were not consonant with those of Akabas. Evidence from many laboratories in many types of ion channels has revealed that the covalent labeling method is a powerful tool to detect conformational changes experienced during the channel gating [114-117; 119; 123]. Akabas suggested that bath-applied thiol reagents such as $MTSES^-$ and $MTSET^+$ can reach cysteines engineered into TM6 that range from the extracellular end to the cytoplasmic end of the pore [126]. In contrast, studies from Smith and coworkers found that two TM6 mutants R334C and K335C (predicted external end) were accessible to SH-modifying reagents, while R347C and R352C (predicted internal end) were either not accessible or lacked significant functional consequences when modified. Covalent modification of R334C increased macroscopic conductance and altered I-V shape due to permeation effects

because modification of R334C increased single channel amplitude without altering P_O [79]. The results of this study are consistent with the hypothesis that in WT-CFTR, R334 occupies a position where its charge can influence the distribution of anions near the outer mouth of the pore. Liu and coworkers have shown that a cysteine engineered in the predicted narrow region of the pore, one turn of the helix from R334 at T338, is also sensitive to pH and to modification by $MTSET^+$ and $MTSES^-$ [128]. In this case, modification with $MTSET^+$ did not increase single-channel conductance, but instead decreased it, due to a blocking effect. These findings are consistent with the notion that T338 is critical for anion permeation and binding, and lies within the pore probably near the narrowest region [47; 49-51; 131].

Most recently, Beck and coworkers reported that there is a conformational change in the extracellular side of the CFTR pore [132]. Using conventional two-electrode voltage-clamp (TEVC) and patch-clamp combined with covalent labeling methods, they found that modification rates of three engineered cysteine residues, I331C, L333C and K335C were 10-100-fold slower in the open state than in the closed state suggesting that there is a conformational changes in a pore-lining helix coupled to CFTR gating [132]. However, they also reported that modification of pore-lining residues 334 and 338 by SH-modifying reagents appeared to be state-independent. In contrast, we report here that modification of R334C appears to be state-dependent. Modification of R334C-CFTR channels by membrane non-permeable SH-modifying reagents is favored strongly by the closed state. This difference might be due to, in large, that in most experiments they used membrane permeant cation and SH-regent MTSEA, which could produce none specific effects as reported previously by Smith *et al*. [79]. It is very likely that this non-specific effect might alter the outcome of the results.

1.9. What forms functional unit of CFTR?

Although it is well established that CFTR functions as small chloride channel; however, neither the number of peptides required, nor the number of pore per functional channel are known. In contrast, the crystal structure of the bacterial ClC channel

confirmed conclusions based on either earlier functional, biochemical, and X-ray studies that the functional cannel is a homodimer and that each of the two monomers contributes a separate pore [133-135]. In bacterial K^+ channel, a homotetramer, each of four monomers contributes to a single, central pore formed at the interface. Several groups attempted to address these questions for CFTR; however, the outcomes are distinctly different. Three alternatives have been proposed (Fig. 22): (i) one-polypeptide/one-pore [83], (ii) two-polypeptides/one-pore [61], and (iii) one-polypeptide/two-pores [136]. One of objectives of this dissertation is to answer this important question (Objective 1).

1.10. CFTR pore is not static

Gunderson and Kopito [39] provided the first tantalizing evidence of subconductance states in WT-CFTR. Using heavily filtered records of channels reconstituted in lipid bilayers, they found that the channels most frequently resided in a subconductance state that represented ~84% of the full conductance state, and that transitions between these states were not random in their order. Their analysis did not include a second subconductance state, perhaps due to the strong filtering applied (10 Hz), although one can be seen in some of their published records. A recent paper from the same group [137] now describes only a smaller subconductance state representing ~38% of the full conductance level, but not the larger subconductance level. Ishihara and Welsh [138] studied WT-CFTR channels in which single-channel records exhibited two open levels that they defined as two open states, *e.g.* O1 (lower amplitude) and O2 (higher amplitude). The poorly-hydrolyzable ATP analog AMP-PNP inhibited the transition from O1 to O2 and prolonged the O1 state. These results suggested that a conformational change occurs in the CFTR pore produced by ATP hydrolysis. Similar results were reported by McDonough et al., in which they found that DPC did not block the major subconductance state of CFTR [76]. Moreover, studies of single CFTR Cl^- channels reconstituted into bilayers revealed evidence of conformational changes in the CFTR pore that were associated with ATP hydrolysis [39; 139]. Zerhusen and Ma [63] reported a single stable subconductance in records from CFTR channels lacking

both the R-domain and NBD2, although the regulation of gating in those dissected channels may not mimic that in WT channels at all. Other investigators have reported that subconductance states were visited more frequently in channels bearing deletions in one of the intracellular loops connecting TM domains, suggesting that these loops may interact with the NBDs to stabilize the open state [140-143], although allosteric effects of these site-directed mutations cannot be ruled out. As mentioned in Conduction Property of CFTR section, CFTR permeates large organic anions when present at the cytoplasmic but not the extracellular side of an excised patch; this asymmetry is dependent upon ATP hydrolysis [49; 50]. This phenomenon may also suggest that there is a link between changes in pore conformation and ATP-dependent gating events at the NBDs.

Several previous studies from our group suggest that the pore does experience a conformational change associated with ATP-dependent gating. A mutant in TM11 (S1118F-CFTR) exhibited alterations in mean bust duration and unitary conductance and macroscopic voltage-jump relaxations, the rate of which was dependent upon the character of the permeating ion, indicating interactions between permeation and gating [144]. This study suggested that the effects of point mutations on gating and permeation may not be mutually exclusive if the residue so mutated lies in the permeation pathway at a position whose conformation changes during gating. A second study described a mutation in TM5 of CFTR (V317E), which resulted in whole-cell currents with marked outward rectification [145]. The greatly decreased single-channel P_O at negative V_M could not be overcome by increased [ATP]. These results suggested that V317 may contribute to, or lie adjacent to, the portion of the CFTR channel that controls access of ions to the permeation pathway (*i.e.* the gate) subsequent to ATP-dependent gating. It is of interest to note that according to a hypothetical model of the pore proposed by McCarty [83], S1118 and V317 occupy roughly homologous positions in TMs 11 and 5, respectively. Fuller *et al.* recently reported that a peptide toxin, GaTx1, inhibits WT-CFTR in a manner of state-dependent which may reflect conformational changes in the pore of CFTR during ATP dependent gating [107].

In addition, two most recent studies also suggest that there is a link between changes in conformation of the CFTR pore and the ATP-dependent gating events at the NBDs. Using the permeant anion $Au(CN)_2^-$ and SH-modifying reagents combined with cysteine substitution approaches, Linsdell and coworker proposed that the conformational changes occurs in TM in advance of channel opening, suggesting that multiple distinct closed pore conformation exist which is tied with intracellular events at the R domain and/or NBDs [146]. Beck and coworkers suggested that ATP binding induces a modest conformational change in the TM6, and this conformational change is coupled to the gating mechanism that regulates ion conduction [132]. The results obtained by these authors are consistent with the notion that the pore of the CFTR channel is dynamic, although there is a conflict result compared to some of our data presented in this dissertation. Nevertheless, there are number of studies suggest that CFTR pore is not static; however, how hydrolysis of ATP at the NBDs induces either the movement of or conformational changes in the membrane-spanning segments (TMs), that leads to opening or closing the channel pore, are not understood. The second objective of this dissertation is proposed to take a first step to probe the dynamic architecture of the CFTR pore using an innovative approach developed for this project.

2. Objectives

The goals of the present study were (1) to determine the oligomeric structure of functional CFTR chloride channel and (2) to probe the dynamic architecture of the outer vestibule of CFTR pore using expression in *Xenopus* oocytes, covalent labeling, and high-resolution electrophysiological analyses.

2.1. To determine what forms the pore of CFTR and how many pores CFTR has?

Single WT-CFTR channels exhibit multiple conductance levels. Although the channel spends the majority of its time shuttling between the main (full) conductance level and the closed level, careful inspection of the fine structure of open-channel bursts led to the observation of two other levels of intermediate conductance. These subconductance levels could represent permeation through completely separate pores, which when summed comprise the full conductance level, or permeation through a single pathway that may reside in multiple configurations differing in conductance. In the first part of this study, we made use of mutants containing cysteines engineered at putative pore-lining positions in TM6 to determine the minimal functional unit of the CFTR channel. These mutants were readily covalently modified by the SH-modifying reagent $MTSET^+$ from the extracellular side (Fig. 5) [79, 147]. First, we used the inside-out single channel recording configuration to study the amplitude and distribution of sub- and full-conductance states of channels before and after modification in single- and double-site mutants. Second, we used the outside-out macropatch configuration to study the kinetics of modification in real time. The results of this study are consistent with a model for the CFTR protein in which a single pore is formed from a single CFTR polypeptide.

2.2. To determine how binding and hydrolysis of ATP at the NBDs controls the conformation of the pore.

As discussed in Section *1.10,* several lines of evidence suggest that the CFTR pore experiences more than two conformations*, i.e.* the closed and open states, including evidence that changes in anion selectivity and susceptibility to blockade are associated with the ATP-dependent gating cycle [39; 49; 50; 76; 86; 136; 139; 144-148]. We found that the stability and frequency of these sub-states are enhanced in some channels bearing mutations in the putative pore-lining regions when we assessed the first objective for this thesis study. Using covalent labeling of channels bearing an engineered cysteine, we demonstrated that the sub- and full-conductance states represent different conducting states of a single chloride-permeation pathway, which may reflect different conformations of the pore-lining helices. In that study, real-time modification of single R334C-CFTR channels was observed during patch clamp experiments by the SH-modifying agent, $MTSET^+$, diffusing to the tip of the electrode; the resulting deposition of positive charge increased the open-channel conductance. Strikingly, we never observed $MTSET^+$-induced modification during an open burst. Therefore, we hypothesized that the accessibility or reactivity of the engineered cysteine in R334C-CFTR for modification by $MTSET^+$ may be favored by the closed state. To test this hypothesis, we performed a series of experiments to measure the rate coefficients for modification by $MTSET^+$ and $MTSES^-$ under a variety of conditions that alter the channel open probability (P_O) of R334C-CFTR. Here we report in the CFTR pore that the rate coefficient for modification of an engineered cysteine by SH-modifying reagents is significantly lower when channels are open compared to when channels are allowed to close. The results provide direct evidence that conformational changes in the outer vestibule of CFTR are linked to the ATP-dependent gating cycle.

3. Methods and Materials

3.1. Preparation of oocytes and cRNA

For mutant R334C, site-directed mutagenesis used a nested PCR strategy in which the mutation was designed into antiparallel oligomers [79]. R334C was prepared from a construct carrying the full coding region of CFTR in the pBluescript vector**.** The rest of the mutants used in this study were prepared with the Quick-Change protocol (Stratagene; La Jolla, CA) using oligonucleotide-mediated mutagenesis**.** All mutant constructs were verified by sequencing across the entire open reading frame before use. WT-CFTR cRNA was prepared from a construct carrying the full coding region of CFTR in the pAlter vector (Promega; Madison, WI). For macropatch recordings, cRNAs were prepared from a high-expression construct, which was kindly provided by Dr. D. Gadsby (Rockefeller University). Oocytes were injected in a range of 5-100 ng of CFTR cRNAs; for experiments using two-electrode voltage clamp (TEVC), CFTR cRNAs were injected along with 0.4 ng of cRNA for the β_2-adrenergic receptor (β_2-AR), allowing activation of CFTR by exposure to isoproterenol in the bathing solution**.** Stage V-VI oocytes were incubated at 18˚C in modified Liebovitz's L-15 media with the addition of N-(2-hydroxyethyl) piperazine-N′-(2-ethanesulfonic acid) (HEPES) (pH 7.5), gentamicin, and penicillin/streptomycin. Recordings were made 24-72 hours after the injection of cRNAs.

3.2. Electrophysiology

For single-channel recording, CFTR channels were studied in excised, inside-out patches at room temperature (22-23°C). Since preliminary experiments showed that the single channel conductance of unmodified R334C-CFTR was very low compared to that of WT-CFTR (Fig. 5) [79, 147], most experiments in this study used asymmetrical [Cl^-] in order to increase the single channel

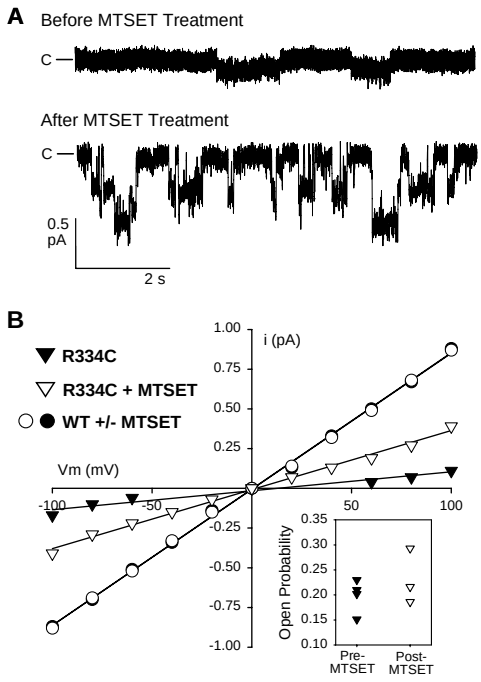

Fig. 5. **MTSET$^+$-induced modification of R334C-CFTR channels. (A)** Records of single channels before and after exposure to MTSET$^+$. **(B)** i/V plots for R334C- and WT-CFTR channels before and after modification by MTSET$^+$. Inset compares P_O in separate patches before and after modification. *Conclusion: Modification increases conductance and does not affect gating in R334C-CFTR.*

amplitude at V_M = –100 mV. Oocytes were prepared for study by shrinking in hypertonic solution (in mM: 200 monopotassium aspartate, 20 KCl, 1 $MgCl_2$, 10 EGTA, and 10 HEPES-KOH, pH 7.2) followed by manual removal of the vitelline membrane. Pipettes were pulled in four stages from borosilicate glass (Sutter Instrument Co.; Novato, CA), and had resistances averaging ~ 10 MΩ when filled with low chloride pipette solution (in mM): 30 NMDG-Cl, 270 NMDG-aspartate, 5 $MgCl_2$, 10 TES (pH 7.4). The SH-modifying reagent MTSET$^+$ (100-200 μM) was backfilled into the pipettes before seal formation and allowed to diffuse to the tip during and after seal formation; solution lacking MTSET$^+$ was used to fill the very tip of the pipette (Fig. 6A). Typical seal resistances were 200 GΩ or greater. Channels were activated by excision into intracellular solution containing (in mM): 300 NMDG-Cl, 1.1 $MgCl_2$, 2 Tris-EGTA, 1 MgATP, 10 TES (pH 7.4), and 50 U/mL PKA. CFTR currents were measured with an Axopatch 200B amplifier (Axon Instruments; Union City, CA), and were recorded at 10 kHz to DAT tape. For subsequent analysis, records were filtered at a corner frequency of 100 Hz and acquired using a Digidata 1322A interface (Axon) and computer at 2.5 ms/point with pClamp 8.0.

For outside-out macropatch recordings, electrode tips were filled with a modified intracellular solution (in mM: 150 NMDG-Cl, 1.1 $MgCl_2$, 2 Tris-EGTA, 10 TES, pH 7.4), and then backfilled with the same solution containing 1 mM MgATP and 100 U/mL PKA. Through time, MgATP and PKA diffused to the intracellular face of the outside-out patch; CFTR channels were fully activated in ~75 min (Fig. 6B). The normal extracellular solution (in mM: 150 NMDG-Cl, 5 $MgCl_2$, 10 TES, pH 7.4) served as bath solution, to which we added $MTSET^+$ or $MTSES^-$ to reach final concentrations of 10-100 µM, respectively. The pipette potential was held at 0 mV and then stepped to either +80 mV or -80 mV during exposure to $MTSET^+$. In the case of modification by $MTSES^-$, the pipette potential was held at 0 mV and then stepped to +80 mV during perfusion of $MTSES^-$. A fast perfusion system (Model SF-77B, Warner Instruments; Hamden, CT) controlled by pClamp software was employed for this set of experiments (bottom panel of Fig. 6); the time resolution of this system is ~ 25 msec as judged by activation of endogenous calcium activated chloride channels (*data not shown*). Outside-out macropatch recordings were performed with an Axopatch 200B amplifier operated by pClamp 8.0 software, filtered at 100 Hz and analyzed using Clampfit 9.0.

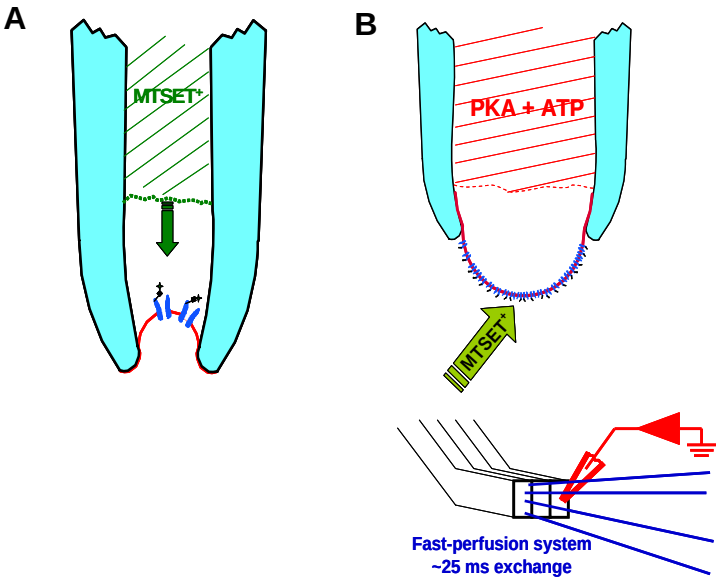

Fig. 6. **Two experimental approaches key to the proposed work. (A)** Excised, inside-out single-channel patches, using real-time modification. **(B)** Excised, outside-out macropatch, with modification induced using a rapid perfusion system.

For TEVC experiments, electrodes were filled with 3 M KCl; individual oocytes were placed in the recording chamber and continuously perfused with ND96 (in mM: 96 NaCl, 2 KCl, 1 $MgCl_2$, and 5 HEPES-NaOH, pH 7.5). For those experiments in which the bath pH was modified, HEPES was replaced by MES (for pH 6.0) or TAPS (for pH 9.0). The different buffers produced no discernible changes in the electrical behavior of WT-CFTR. TEVC data were generated using a GeneClamp 500 amplifier (Axon), and pClamp 8.0 at room temperature (21-24°C). The volume of the perfusion chamber used in this study was about 100 μL and the flow rate to the chamber was ~ 6 mL/min. The membrane potential was held at -30 mV and then ramped from -80 mV to +60 mV in a period of 200 ms in order to construct whole cell I-V plots. Conductance was calculated from the slope of the I-V plot at the reversal potential (E_{rev}).

3.3. Analysis of single channel experiments

The Fetchan and pSTAT programs of pClamp 8.0 were used to calculate open probability (P_O) and to make all-points amplitude histograms for R334C-CFTR channels before and after modification. Referenced to a midpoint between the last unmodified and the first modified channel openings, paired records lasting ~240 seconds were analyzed for both unmodified and modified channels in order to avoid errors due to effects of dephosphorylation**.** Prior to analysis, the single channel traces were further filtered to 75 Hz and the baseline-shifts in some records were corrected manually using pClamp 8.0 or 9.0. Different open (**s1, s2 and f)** and closed levels were first identified manually by the cursors and subsequently all-point histograms were constructed. Only records from patches with low noise, and which apparently only contained one active channel, were used for amplitude analysis. The all-points amplitude histograms were fit using multiple Gaussians and optimized using a simplex algorithm. As described below, R334C channels exhibit multiple conductance levels, with **s1** = subconductance level 1, **s2** = subconductance level 2, and **f** = full conductance level, as well as the closed level (**c**) (see Fig. 7). The proportion of time spent in each conductance state was determined from the fit results (*see* Fig. 9G). For the purpose of this study, open probability (P_O) was defined according to Eq. 1 as:

$$P_O = \frac{A(s1) + A(s2) + A(f)}{A(T)} \qquad \text{Eq. 1}$$

where each term is the fraction of the total (T) area contributed by each open level (**s1**, **s2**, and **f**) to the Gaussian curves fit to amplitude histograms generated before and after modification. All single channel records presented in this study, before and after modification by $MTSET^+$, were paired experiments. It is noteworthy that because the single channel amplitude of R334C is very small, we transferred the all-points histogram data for R334C-CFTR channels to PeakFit v. 4.11 (SYSTAT Software Inc.; Chicago, IL) to verify the result of fits in pClamp 8.0.

3.4. Analysis of macropatch experiments

For outside-out macropatch data, we used pClamp 9.0 to fit the time-course of covalent modification of CFTR currents using an exponential function to obtain the time constant, τ, which was converted to a rate coefficient with units of $sec^{-1}M^{-1}$ by dividing by $[MTSET^+]$ or $[MTSES^-]$. In all experiments, we compared the quality of the fit of the data by a single exponential function and the fit by the sum of two exponentials by assessing the values of the correlation coefficient and standard deviation, as well as by visual inspection of the goodness of fit to the data trace itself. For those experiments where the data were described best by a single exponential function (Figures 16A, 18B, and 19A), fitting the data with the sum of two exponentials led to no improvement of fitting results. For those outside-out macropatch experiments where CFTR channels were exposed to $MTSET^+$ twice (*see* Fig. 12), we determined the relationship between the magnitude of the fractional increase in current upon first exposure (fractional ΔI), and the rate coefficient for $MTSET^+$ modification during the second exposure (k_2, equals converting time constant (τ_2) at the second exposure to a rate coefficient with units of $sec^{-1}M^{-1}$ by dividing by $[MTSET^+]$)*)*. Fractional ΔI upon first exposure was calculated as A/(A+B), where A represents the macroscopic current increment resulting

from the first $MTSET^+$ modification, and B is the macroscopic current increment from the second $MTSET^+$ modification.

3.5. Source of reagents

Unless otherwise noted, all reagents were obtained from Sigma Chemical Co. (St. Louis, MO). $MTSET^+$ $MTSES^-$ were purchased from Toronto Research Chemicals Inc. $MTSET^+$ and $MTSES^-$ were first suspended in deionized water at a concentration of 100 mM, frozen in aliquots at – 20°C, and thawed and diluted into recording solution immediately before use. L-15 media was from Gibco/BRL (Gaithersburg, MD). PKA was from Promega.

3.6. Statistics

Unless otherwise noted, values given are mean ± SEM. Statistical analysis was performed using the *t*-test for unpaired or paired measurements by Sigma Stat 2.03 (Jandel Scientific; San Rafael, CA), with $p < 0.05$ considered indicative of significance.

4. Results

4.1. To determine what forms the pore of CFTR and how many pores CFTR has

4.1.1. Wildtype and mutant CFTRs exhibit comparable subconductance states with differing stability and probability of occurrence

CFTR channels have been reported to exhibit subconductance states [39; 60; 76; 86; 136; 138; 143; 150]. In our recordings of WT-CFTR single-channel currents from detached inside-out patches, subconductance states, although clearly discernable, were rare events, occurring in only 20% of bursts. For the purposes of this study we defined a subconductance state as a conductance level that was visited during many open-channel bursts, and which was sufficiently stable to be recognized in an all-points histogram [151; 152]. By careful, manual evaluation of the fine-structure of open-channel bursts, multiple conductance levels of WT and mutant CFTRs were easily identified in patches containing 1-2 channels. Conductance levels thus identified were then confirmed using all-points amplitude histogram analysis; sojourns at these current levels are readily detectable by pClamp so that this operational definition permits an unambiguous separation of subconductance events from other small, non-CFTR single-channel events that contaminate some records.

Fig. 7 contains an example of the subconductance behavior of WT-CFTR recorded in a detached patch bathed by symmetrical 150 mM [Cl^-]. Three states that differ in conductance are discernable: 7.8 pS, referred to here as the full conductance state **(f)**, and two subconductance states of 5.3 and ~3 pS, referred to as **s2** and **s1** respectively. The dominant single-channel current in WT-CFTR is the full conductance state, *i.e.* transitions between **c** and **f** levels in Fig. 7A. The vast majority of WT-CFTR openings exhibit transitions from **c** directly to **f**, and back again, without sojourns in subconductance states.

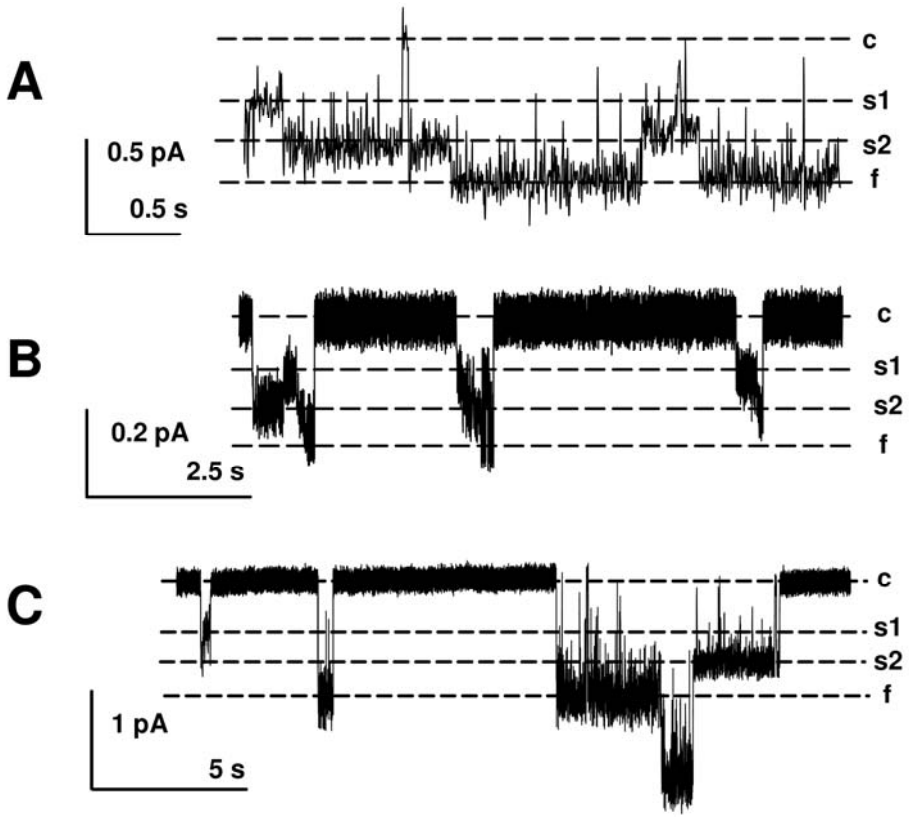

Fig. 7. **Sample traces of CFTR channel openings.** Each current level is indicated by a dashed line; **c**, **s1**, **s2** and **f** represent current levels of the closed, subconductance level 1, subconductance level 2 and full-conductance states, respectively. **(A)** WT-CFTR channel recorded with symmetrical ~150 mM [Cl^-]. **(B)** and **(C)** Records for R334C-CFTR and T338A-CFTR, respectively, were generated with asymmetrical [Cl^-] where the pipette was filled with 30 mM [Cl^-] and bath (cytoplasmic) solution contained 300 mM [Cl^-] in order to potentiate the single channel amplitude. Traces A and C were filtered at 400 Hz; whereas trace B was filtered at 100 Hz. All traces were recorded at V_M = -100 mV.

Fig. 7 also contains records illustrating the subconductance behavior of two mutant CFTRs: R334C and T338A. R334C-CFTR exhibits a full conductance that is less than that of the wild type under comparable conditions [79] (also see Fig. 5) and T338A-CFTR exhibits an increased full conductance (~9.8 pS in T338A-CFTR with symmetrical 150 mM chloride). Despite these differences in full conductance, however, the *relative* amplitudes of the three conductance states for WT-CFTR and the two mutants are quite similar, *i.e.* **s1** is ~40% of **f**, and **s2** is ~70% of **f**. The **s2** subconductance of WT- CFTR was previously reported by Gunderson and Kopito [39] to reflect ~84% of the full conductance level, measured under conditions different from

ours; they did not identify other subconductance levels in their data, perhaps because the data were filtered heavily.

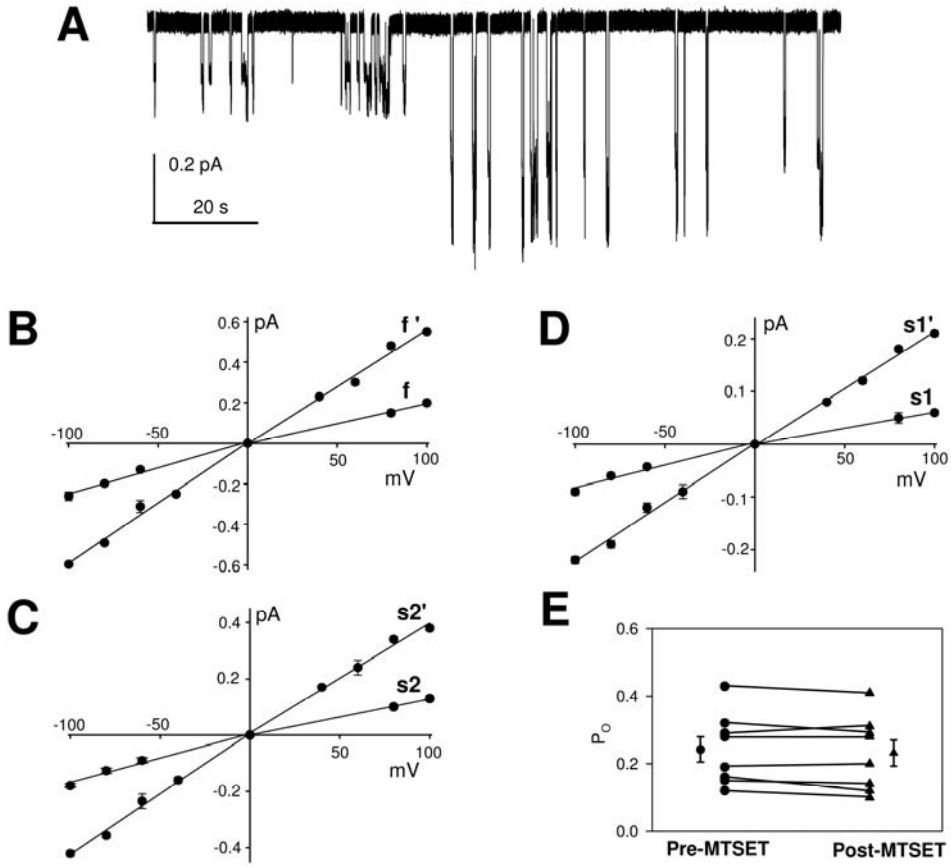

Fig. 8. **Representative trace from an oocyte expressing R334C-CFTR in the detached, inside-out patch configuration; V_M = -100 mV, with asymmetrical [Cl^-].** The pipette was backfilled with solution containing 200 μM $MTSET^+$. After excision, 1 mM MgATP and 50 U/mL PKA were applied to the intracellular solution. CFTR channels were monitored through time; over the course of 10-15 minutes, the channel was modified by $MTSET^+$ diffusing into the tip of the patch pipette, as indicated by the increase in the single-channel amplitude. The trace was filtered at 75 Hz. **(B-D)** Current-voltage relations for the s1, s2, and f conductance levels before (labeled **s1**, **s2**, and **f**) and after $MTSET^+$-induced modification (labeled **s1'**, **s2'**, and **f'**), measured with symmetrical ~200 mM [Cl^-]. **(E)** Open probability (P_O) determined before (filled circles) and after (filled triangles) covalent modification by $MTSET^+$ for eight paired patches containing single R334C-CFTR channels. Each value represents mean P_O over ~ 4 minutes before and after modification, which was assumed to have occurred at the midpoint between the last unmodified and first modified openings. The two isolated symbols (filled circle and triangle with error bars) are the mean (± SEM) P_O values for records pre- and post-modification by $MTSET^+$.

This result suggests that neither the R334C nor T338A mutation, although they involve residues reported to lie within the CFTR pore [7, 79], greatly altered the *relative* magnitude of the subconductance states. The subconductance states seen in the mutant channels, however, differed markedly in their stability and probability of occurrence from that seen in WT-CFTR. In a longer record of single-channel currents from oocytes expressing R334C-CFTR (Fig. 8A), the most prominent state (with a conductance of 1.5 pS) corresponds to the s2 subconductance level that was reported previously (Fig. 5) [79], although upon closer examination of the fine structure of the open bursts, it is found that within nearly every burst there are transitions to three conductance states: one lower in conductance than that of the most frequent state and one higher in conductance. These results suggest that amino acid substitutions in TM6 alter the relative occurrence of subconductance states, but not their relative amplitude in relation to the full conductance state, as if at least some portion of the conduction path for the three states (**s1**, **s2**, and **f**) is shared.

4.1.2. Deposition of a positive charge at 334 amplifies all conductance states proportionately

We reasoned that if the three conductance states reflect different behaviors of a shared portion of the conduction path, which includes the amino acid at position 334 in TM6, it would be possible to use the properties of the R334C mutant to investigate the architecture of the functional CFTR pore. We showed previously that covalent modification of R334C-CFTR channels with $MTSET^+$ increased the amplitude of the most prominent single-channel conductance (referred to here as **s2**) without altering gating (Fig. 5) [79]. In our previous experiments, we assayed the impact of $MTSET^+$-induced chemical modification in two ways, by comparing single-channel amplitudes in patches detached from different oocytes, either untreated or exposed to $MTSET^+$ prior to recording (Fig. 5), and by monitoring the modification of single channels in real-time using recording pipettes backfilled by $MTSET^+$ (*see* Methods). In the present experiments, we monitored modification in real-time to increase the likelihood that we

would be able to observe the consequences of the reaction while in progress [116]. The record in Figures 8A and 9A are representative of such experiments. Electrode tips for these inside-out recordings were backfilled with solution containing 200 μM $MTSET^+$. R334C-CFTR chloride channels were modified in ~15 min by $MTSET^+$ diffusing down the electrode tip as reflected by an increment of **s1**, **s2** and **f** conductance levels ~ 2.1- to 2.3-fold. We analyzed eight paired, inside-out single channel records (both pre- and post-modified channels included in the same patch) that contained only one R334C-CFTR channel per patch, as shown in Figs. 8A and 9A. In every case *only a single modification event was ever observed*. Furthermore, all of the subconductance states appeared to be modified simultaneously. We maintained the patches that contained modified R334C-CFTR channels for up to 45 min in some experiments, and found that following modification by $MTSET^+$, the amplitudes of the **s1**, **s2** and **f** conductance states consistently stayed at the same level, with no further modification observed.

The all-points histograms in Figs. 9D and 9E, compiled by analyzing periods of four minutes immediately before and after the single modification event, confirm that the amplitudes of all three conductance states were increased by chemical modification. Furthermore, the mean values compiled in Table 1 indicate that the amplitude of each conductance state increased in approximately the same proportion, between 2- and 2.3-fold (*see also* Fig. 9F). Covalent modification by $MTSET^+$ did not change the apparent reversal potential for either subconductance state or the full conductance state, but only increased the slope conductance of each state (Fig. 8B-D). Hence, the shared impact of covalent modification by $MTSET^+$ on the amplitude of all conductance states exhibited by R334C-CFTR channels was also consistent with the hypothesis that the three conductance states have at least a portion of the conduction path in common.

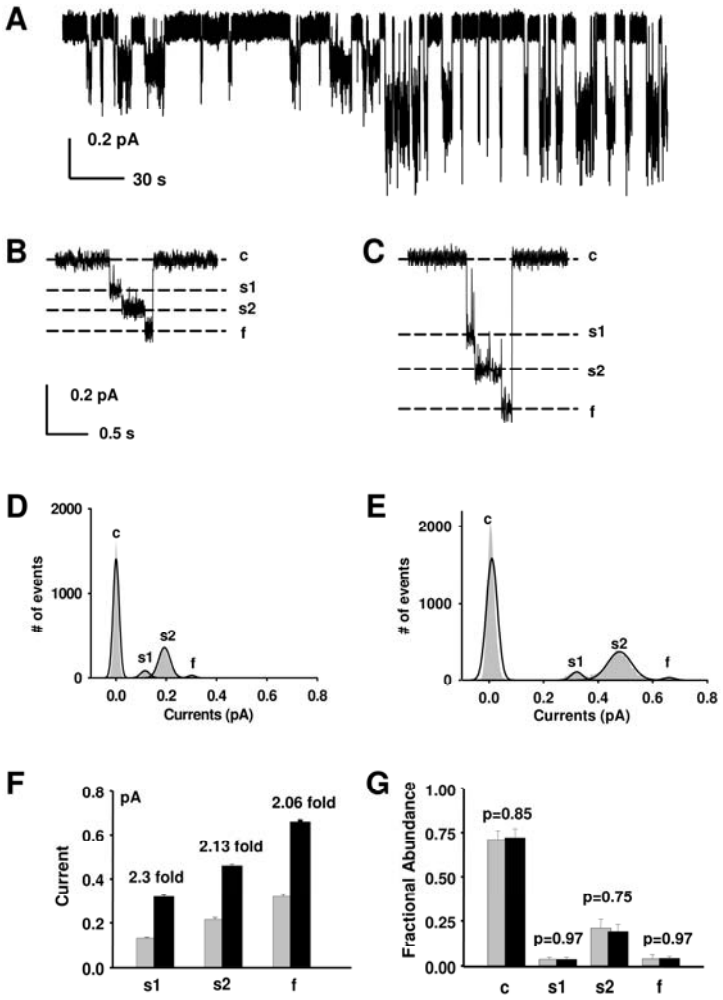

Fig. 9. **(A)** A representative experiment for R334C-CFTR, using experimental conditions identical to those in Fig. 8A. **(B, C)** Two isolated single bursts representing R334C-CFTR from the same patch before (B) and after (C) modification by $MTSET^+$. Each current level is indicated by dashed lines drawn by eye. **(D)** An all-points amplitude histogram representing the single channel amplitude of each state before modification by $MTSET^+$. There are four current levels indicating the closed (**c**), **s1**, **s2**, and **f** states. The solid lines are fit results by PeakFit v. 4.11 to a Gaussian function. The values for **s1**, **s2** and **f** were 0.14 pA, 0.21 pA and 0.32 pA, respectively, in this experiment. **(E)** Representative all-points amplitude histogram of each state after modification by $MTSET^+$. The values for modified **s1**, **s2** and **f** were 0.31 pA, 0.46 pA and 0.66 pA, respectively, in this experiment. **(F)** The unitary current values of each conductance state, as determined from all-points amplitude histograms as shown in (D). Gray and black bars indicate averaged unitary current values of pre- and post-modified channels, respectively (n = 8) The **s1**, **s2** and **f** levels were increased by the same degree upon modification by $MTSET^+$. **(G)** Summarized fractional abundances of each conductance state and closed state representing the data from eight paired experiments. Gray and black bars indicate data before and after modification by $MTSET^+$, respectively. Comparisons between pre- and post-modification values were done by paired *t*-test; p-values are indicated.

Table 1. Effects of $MTSET^+$-induced modification on permeation and gating.

Mutants	P_O	P_O'	s1 (pA)	s1′ (pA)	s2 (pA)	s2′ (pA)	f (pA)	f′ (pA)
R334C	0.24 ± 0.04	0.23 ± 0.04	0.13 ± 0.01	0.32 ± 0.01*	0.22 ± 0.01	0.46 ± 0.01*	0.32 ± 0.01	0.66 ± 0.01*
R334C/T338A	0.26 ± 0.04	0.25 ± 0.04	N/A	N/A	N/A	N/A	0.48 ± 0.01	0.96 ± 0.01*

P_O, **s1**, **s2**, and **f** indicate the open probability, subconductance level 1, subconductance level 2, and full-conductance states, respectively, for channels before $MTSET^+$ modification. Parameters with prime notation (P_O', **s1**′, **s2**′, and **f**′) are representative of channels after $MTSET^+$ modification. For R334C-CFTR, n = 8 paired experiments; for R334C/T338A-CFTR, n = 3 paired experiments. All experiments were recorded at V_M = -100 mV. Values are mean ± SEM. * indicates significant difference compared to pre-modification values.

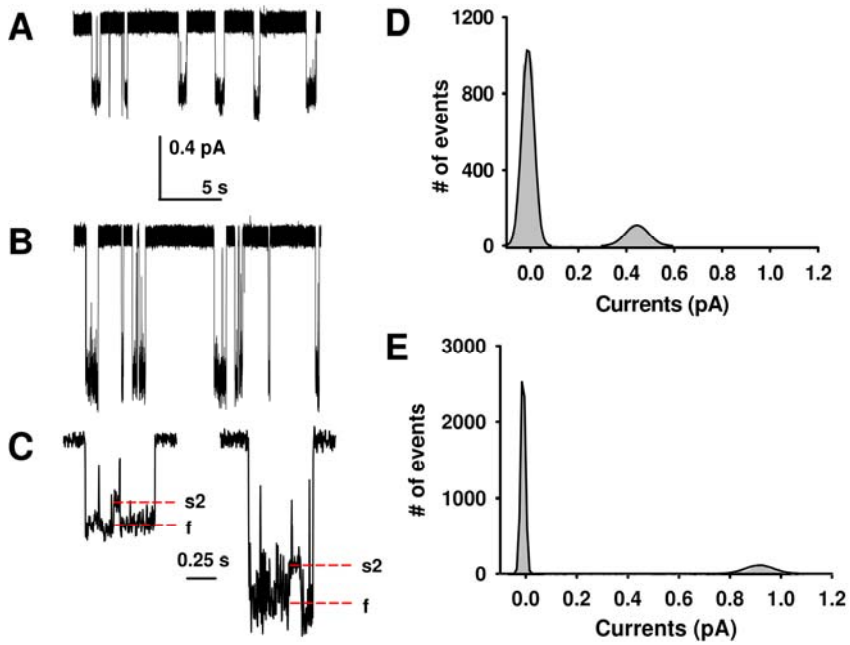

Fig.10. **(A**, **B)** Representative traces of R334C/T338A-CFTR before and after modification by $MTSET^+$, from the same patch, using experimental conditions identical to those in Fig. 9. **(C)** Expanded traces showing the **s2** and **f** conductance levels before and after modification. The **s2** conductance level increased from 0.35 to 0.72 pA in the bursts shown. **(D**, **E)** All-points amplitude histograms corresponding to the traces shown in (A) and (B). Solid lines indicate fits to the Gaussian function. The amplitudes of the full-conductance state for pre- and post-modified channels in this individual experiment are 0.49 pA and 0.98 pA, respectively. All records were filtered at 75 Hz.

Because the single-channel conductances of R334C-CFTR channels are relatively low, we also explored the impact of covalent modification of a double mutant, R334C/T338A, that exhibits an increased single-channel conductance. The subconductance states of R334C/T338A-CFTR were, however, very brief and unstable compared to those of R334C-CFTR (Fig. 10). While it was possible to visually identify a subconductance level corresponding approximately to the **s2** level (~70% of f, Fig. 10C), inspection of multiple bursts suggested the presence of an **s1** state, even less stable than **s2**, which could not be characterized with certainty due to its brief duration and rare occurrence. All-points amplitude histograms (Fig. 10D) indicated only two amplitude levels (*i.e.* closed and open states) in the double mutant. The extreme brevity of the two subconductance states in this mutant result in these states not being represented in the amplitude histograms, because this analysis mode is

heavily weighted toward frequent or prolonged events. The amplitude of the full-conductance state of R334C/T338A-CFTR was larger than that of R334C by ~50% at V_M = –100 mV under identical experimental conditions. The amplitudes of the brief subconductance states and the full-conductance state were increased ~2-fold upon $MTSET^+$-induced modification (Fig. 10C, E, and Table 1). There were no further changes in amplitude of R334C/T338A-CFTR channels after the first modification event detected. Hence, the behaviors of the two detectable conductance states in this dual mutant were enhanced by treatment with $MTSET^+$ in a manner identical to that seen in R334C-CFTR. It is not clear why addition of the T338A mutation destabilizes the subconductance states that are made prevalent by the R334C mutation, but these results are consistent with the general finding that mutations in TM6 alter the prevalence of substates but not their relative amplitudes. Furthermore, while the identification of subconductance levels was tentative in WT-CFTR due to their rarity, the consistency of the relative amplitudes in unmodified R334C- and R334C/T338A-CFTR channels, and their amplification upon chemical modification, confirm that the substates represent a feature of the CFTR conduction process.

4.1.3. Covalent modification of R334C-CFTR did not alter gating

We previously reported that modification of R334C-CFTR by $MTSET^+$ did not alter gating as defined by comparing open probability in patches from treated and untreated oocytes as well as that of channels monitored during the process of modification (Fig. 5) [79]. Analysis of the subconductance behavior of R334C-CFTR provided an opportunity to re-examine the question of possible gating effects by asking whether modification of R334C-CFTR channels by $MTSET^+$ altered the prevalence or duration of the three conductance states. As described in Materials and Methods we calculated values for open probability (P_O) according to the distribution of the times spent in each conductance state derived from the amplitude histograms. The overall P_O of R334C-CFTR channels before and after $MTSET^+$ modification was 0.24 ± 0.04 and 0.23 ± 0.04, respectively (p = 0.91; *see* Table 1 and Fig. 8E). Furthermore, as shown in Fig. 9G, the fractional abundance of the **s1**, **s2**, and **f** conductance states did not change upon $MTSET^+$-induced modification in R334C-CFTR channels. $MTSET^+$-induced

modification was without effect on the P_O of R334C/T338A-CFTR channels (Table 1). These results confirm and amplify our previous findings that covalent modification at the 334 locus alters the conduction properties of CFTR but is without effect on channel gating or channel number [79; 152]. In contrast, modification of engineered cysteines in ClC-0 channels affected both conduction and gating [153]. Furthermore, the observation in R334C-CFTR that the amplitudes of the **s1**, **s2** and **f** states increased by an equivalent proportion, and apparently simultaneously, upon modification by $MTSET^+$ suggests that each of these states reflects the activity of a single pore, or a portion of a shared conduction pathway, rather than the activity of two separate pores. Miller and coworkers [134], in contrast, showed that modification of cysteines substituted in ClC-0 channels occurred in two steps, as predicted for a dimeric, two-pore structure containing multiple targets for cysteine modification.

4.1.4. How many cysteines in one pore?

If the portion of the conduction path occupied by R334 is common to all three conductance states, the question remains: How many of these arginine residues are present in the functional pore of WT-CFTR? In other words, is the single common pathway formed from a single CFTR polypeptide or are perhaps two polypeptides required, each contributing a single R334? If each CFTR pore contained two copies of R334, then the process of covalent modification should, in principle, proceed in two steps coinciding with the serial modification of the two cysteines. As described above, however, we were never able to observe more than a single modification event in single-channel experiments. In addition, despite many hours of recording, we were never able to observe the process of modification occurring while a channel was in the open state. In all cases the modification event appeared to have occurred during an inter-burst closed interval so that we could not eliminate the hypothesis that the modification reaction occurred in two steps. A similar result was obtained using a double mutant, R334C/K1250A, that exhibits a prolonged open state duration (Fig. 15B). This observation suggests that modification at this site may be favored by the closed state.

To investigate the number of cysteines per pore we examined the time course of the modification of CFTR channels by $MTSET^+$ in outside-out macropatches using a rapid perfusion system. We reasoned that if attaining the full conductance state required the modification of more than one cysteine, the kinetics of modification might be expected to reflect this. For example, it seemed likely that the change in local electrostatic potential caused by the modification of one cysteine [79] would significantly alter the thiol-disulfide exchange reaction at the second cysteine by two mechanisms that might partially cancel. A positive local electrostatic potential would tend to reduce the local concentration of the $MTSET^+$, but it would also shift the pKa of the target cysteine to more acidic values, rendering it more reactive [155-157].

Following activation of channels by diffusion of PKA and ATP into the patch from the pipette, a rapid perfusion system was used to apply $MTSET^+$ to the extracellular surface of the patch. In Fig. 11, activated R334C-CFTR channels were first exposed to the bath solution containing no $MTSET^+$ for a time period of ~20 sec, and then perfused by bath solution containing 50 μM $MTSET^+$. R334C-CFTR macroscopic current increased rapidly, reflecting modification by $MTSET^+$ [78]. The final, steady-state macroscopic current amplitude of modified R334C-CFTR was increased by 2.3 ± 0.22 fold after prolonged exposure to 50 μM $MTSET^+$. This is consistent with the results of single-channel recordings, and is further evidence that $MTSET^+$-induced modification does not change P_O because the increase in macropatch current can be fully explained by the increase in single-channel amplitudes (Fig. 9F). More importantly, the kinetics of the modification process were fit best with a single exponential function in all five experiments (*e.g.*, red line in Fig. 11A). The mean value of the time constant describing this relaxation (τ) was 2.37 ± 0.24 sec (n = 5). The half-time for solution change was on the order of 0.025 sec (*see* Methods) so the observed time course must reflect the kinetics of the reaction of $MTSET^+$ with the target thiol.

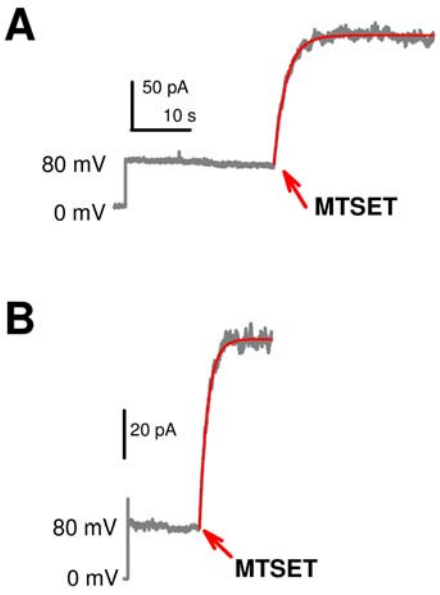

***Fig.11.* Outside-out macropatch experiments for mutants R334C- and R334C/K335A-CFTR.** The pipette potential was held at 0 mV, and then stepped to +80 mV. Arrows indicate the rapid application of $MTSET^+$ to the outside surface of the patches. **(A)** An example of macroscopic current of R334C-CFTR, filtered at 200 Hz. The red line indicates the curve fit by a single exponential function with $\tau = 2.2$ sec in this individual experiment. The amplitude of macroscopic current was increased by 2.8-fold upon modification by $MTSET^+$ in this experiment. **(B)** Representative macroscopic current of R334C/K335A-CFTR; red line is the curve fit, with $\tau =$ 1.1 sec in this experiment.

Previous studies from our laboratories provided evidence that both R334 and K335 contribute to the development of a positive electrostatic potential in the outer vestibule of CFTR [79]. This provided an opportunity to test directly the notion that a nearby positive charge would modify the rate of modification of the cysteine at 334 by comparing the rate of modification of R334C-CFTR with the rate of modification of R334C/K335A-CFTR (Fig. 11B). The amplitude of macroscopic current was increased 2.97 ± 0.24 fold by 50 μM $MTSET^+$ in R334C/K335A-CFTR. The kinetics of current increase were fit best with a single exponential function in each patch (red line in Fig. 11B), and the mean value of τ was decreased to 1.25 ± 0.11 sec ($n = 4$). These data are compatible with the notion that the rate of modification of a cysteine at position 334 is sensitive to the local electrostatic potential, partially determined by the amino acid at position 335, although we cannot discount the possibility that the K335A mutation altered the pore structure in the vicinity of R334C. We have also recently found that the rate of modification of a cysteine engineered at T338, predicted to lie one helical turn cytoplasmic to position R334, is sensitive to the charge at position 334 [155].

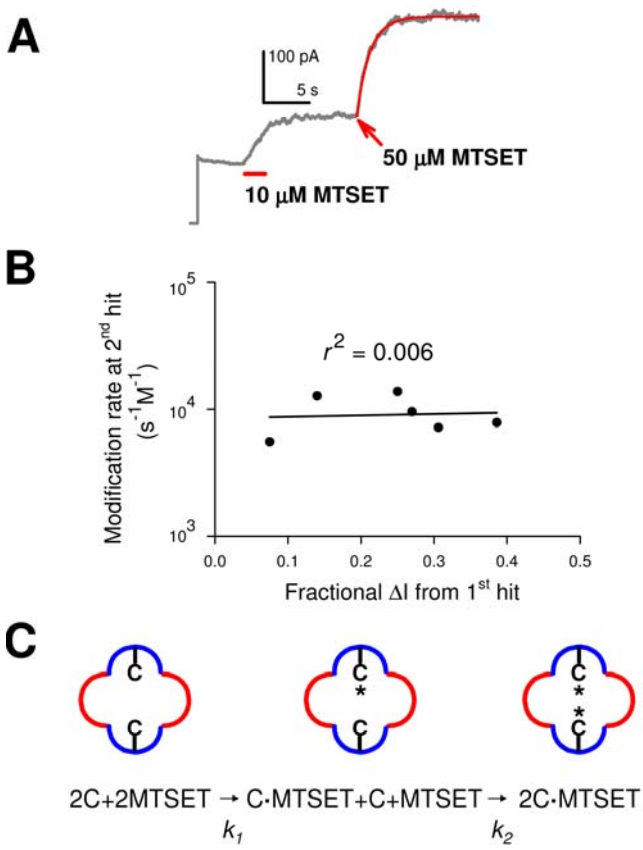

Fig.12. **(A)** Outside-out macropatch for R334C-CFTR, using a protocol similar to that shown in Fig. 11 but with two exposures to $MTSET^+$. The patch was first exposed to the solution containing 10 μM $MTSET^+$ for 2.5 sec (red bar), then to the solution containing no $MTSET^+$ for 10 sec, and finally to the solution with 50 μM $MTSET^+$ (arrow). The second modification in the presence of 50 μM $MTSET^+$ was best described by a single exponential function indicated by a red line, with $\tau = 2.18$ sec. **(B)** The rate coefficient of modification upon second exposure to $MTSET^+$ (50 μM) was plotted *vs*. the fractional change in current (Δ I) from the first modification due to brief exposure to a low dose of $MTSET^+$; data points were fit by linear regression, $r^2 = 0.006$. **(C)** Three proposed configurations for the structure of CFTR channels formed by a dimer of polypeptides (top). As shown in (A), brief exposure to 5-10 μM $MTSET^+$ should modify a subset of the available cysteines resulting in one of three conditions: 1) in some R334C-CFTR pores, neither of the cysteines would be modified; 2) in some pores, only one cysteine would be modified; and 3) in some pores, both of the two cysteines within a single pore would be modified (stars indicate the cysteines that were modified by $MTSET^+$). In the bottom panel, a reaction scheme is proposed that would describe sequential modification of two engineered cysteines in each pore. Due to the electrostatic effects of modification by $MTSET^+$, we anticipate that the two rate coefficients, k_1 and k_2, would be different. Under these mixed conditions, the kinetics of the macroscopic current increase during the second $MTSET^+$-induced modification should no longer be described by a first-order exponential function.

As an additional test for the presence of multiple cysteines we studied the kinetics of modification of R334C-CFTR channels in outside-out macropatches using a two-pulse protocol as follows: solutions used for perfusion contained 5-10 μM $MTSET^+$ for 2.5 sec, then zero $MTSET^+$ for 10 sec, and finally 50 μM $MTSET^+$ until the current increased to a new steady-state level (Fig. 12A). Upon brief exposure to a relatively low concentration of $MTSET^+$, the amplitude of the macroscopic current was increased by a small fraction; the macroscopic current amplitude increased rapidly upon the second prolonged application of 50 μM $MTSET^+$. The magnitude of the *total* increase in conductance with the dual exposure protocol was the same as with the single-exposure protocol (2.35 ± 0.27 fold). Hence, the brief exposure to $MTSET^+$ resulted in modification of a subset of the available cysteines. Most importantly, the kinetics of the second modification were fit best by a single exponential function having $\tau = 2.35 \pm 0.32$ sec (n = 6), virtually identical to that seen in experiments using the single exposure protocol ($\tau = 2.37 \pm 0.24$ sec, p = 0.891).

We reasoned that if two cysteines in each channel must be modified to attain the complete conductance change, then there might be a relationship between the fraction of cysteines modified in the first exposure and the rate of modification of the remaining cysteines in the second exposure to $MTSET^+$. If there were two cysteines in each one-pore CFTR, then following the first brief exposure to $MTSET^+$ at a low concentration the pool of R334C-CFTR channels should comprise a mixed population of unmodified, singly modified, and doubly modified channels (Fig. 12C); longer exposure to $MTSET^+$ in the first treatment would lead to a greater increase in current, due to modification of more cysteines. The change in electrostatic potential due to modification of one cysteine would be expected to alter the rate of modification of the remaining cysteine, as suggested by the difference in response in R334C- and R334C/K335A-CFTR. Fig. 12B contains a plot of the modification rate coefficient (k_2) during the second exposure to $MTSET^+$ as a function of the fractional change in current resulting from the first exposure to $MTSET^+$ (*see* Methods). It can be seen that there was no relationship between the magnitude of the increase in current upon first exposure, relative to the total increase in current, and the rate of modification during the second exposure. The modification rate coefficient, k, in experiments with the single exposure protocol, such

as in Fig. 11A, and the modification rate coefficient, k_2, in experiments with the two-pulse exposure, such as in Fig. 12A, were 8,569 ± 518 $sec^{-1}M^{-1}$ (n = 5) and 9,142 ± 863 $sec^{-1}M^{-1}$ (n = 6), respectively (p = 0.561). Hence, the data do not support the presence of a mixed population of channels with multiple cysteine targets, but rather support a model in which each one-pore CFTR contains a single cysteine at 334.

4.1.5. Does modification of one cysteine absolutely prohibit modification of a second cysteine in the same pore?

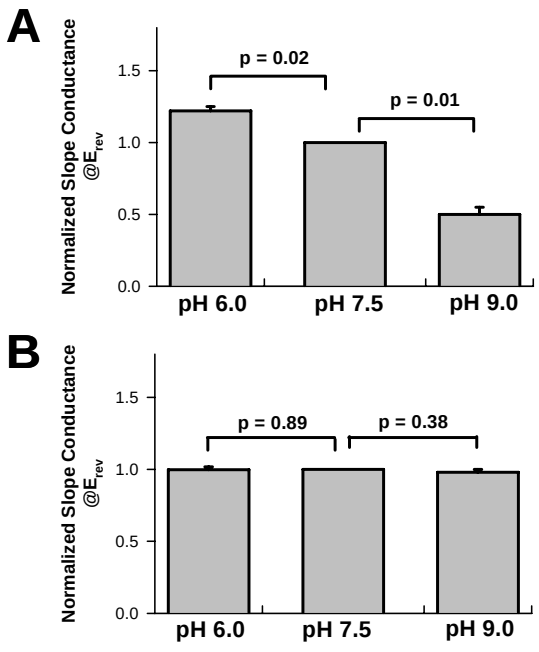

Fig. 13. **R334C-CFTR was not accessible to protons after modification by $MTSET^+$. (A)** Oocytes expressing R334C-CFTR and β_2-AR were first activated by ND96 plus 5 μM isoproterenol at pH 7.5 for 6 min. Following activation, bath pH was then changed to either pH 6.0 or pH 9.0, then to pH 7.5. On average the macroscopic conductance of R334C-CFTR increased 22 ± 3% (p = 0.02, n = 3) in pH 6.0 and decreased 50 ± 5% (p = 0.01, n = 3) in pH 9.0. **(B)** Oocytes expressing R334C-CFTR and β_2-AR were first activated by ND96 plus 5 μM isoproterenol at pH 7.5 for 6 min and then followed by the same solution containing 200 μM $MTSET^+$ for 4 min; the macroscopic conductance was increased by ~ 2.5-fold upon application of $MTSET^+$ (*data not shown*). Modification by $MTSET^+$ prevented the pH-induced response seen in R334C-CFTR macroscopic conductance.

Our interpretation of the preceding set of experiments rests on the assumption that modification of one cysteine by $MTSET^+$ would not simply prevent modification of a second, nearby cysteine due to an absolute steric/electrostatic block of the access pathway. To determine if any engineered cysteines remain unmodified in R334C-CFTR channels after prolonged exposure to $MTSET^+$, we took advantage of the sensitivity of

unmodified cysteines to bath pH. R334C-CFTR channels were examined by TEVC, and channels were activated via the β_2-AR by exposure to isoproterenol. As reported previously, the conductances of oocytes expressing unmodified R334C-CFTR channels were sensitive to bath pH, due to titration of the partial negative charge on the unmodified cysteine [79].

Acidifying the bath pH from 7.5 to 6.0 increased the macroscopic conductance while alkalinizing the bath pH to 9.0 decreased the macroscopic conductance (Fig. 13A). In three paired experiments, the macroscopic slope conductance at the reversal potential (g @ E_{rev}) increased on average 22 ± 3% (p = 0.02) at pH = 6.0, and decreased 50 ± 5% (p = 0.01) at pH = 9.0. The macroscopic conductance of R334C-CFTR was increased ~ 2.5-fold (n = 3, *data not shown*) upon $MTSET^+$-induced modification at bath pH 7.5, which is consistent with our previous report [79]. However, after R334C-CFTR channels were covalently modified by 200 μM $MTSET^+$, the macroscopic conductance was no longer sensitive to pH titration (Fig. 13B). If an unmodified cysteine remained within the pore of channels that had been previously exposed to $MTSET^+$, macroscopic conductance should remain sensitive to pH, although the pKa might be shifted in the acidic direction due to the effect of the nearby positive charge [155-157]. These results indicate that all engineered cysteines in the CFTR pore were modified by $MTSET^+$ during a single exposure, consistent with formation of the channel pore by a single CFTR polypeptide.

The possibility remains, however, that two separate copies of R334C contribute to each functional pore, and that $MTSET^+$-induced modification of these two targets occurs with identical rates as expected if the two sites are far enough apart in the folded channel polypeptide that the electrostatic charge change that accompanies modification of one site is not sensed at the other site. In this case, the ~2.5-fold change in conductance between unmodified and modified channels would represent the summed effects of two modification events per channel. One strong argument against this model exists in the fact that we never saw two-step increases in single-channel current during real-time modification experiments, despite many hours of observation.

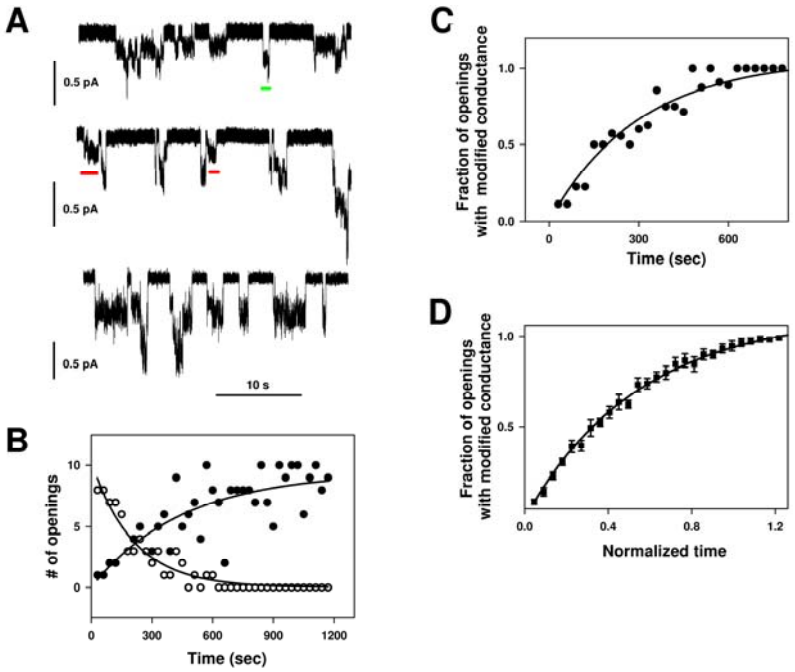

Fig.14. (**A)** An individual patch containing at least three active R334C-CFTR channels. Upper trace includes the first modified R334C-CFTR opening, indicated by the green bar. Through time, the number of unmodified R334C-CFTR openings was reduced (middle trace, labeled by red bars), and finally all openings exhibited the modified conductance (bottom trace). **(B)** The number of unmodified openings (open circles) and modified openings (filled circles) within successive 30-second periods, plotted as a function of time. Two solid lines indicate the fit of modified and unmodified openings using an exponential rise function and an exponential decay function, respectively. **(C)** The fraction of openings that are modified (the number of modified openings divided by the total number of openings during that time period) as a function of time, for the individual experiment shown in Panel A. The data were fit with an exponential function (solid line). **(D)** Normalized responses in six multichannel patches. Records were normalized with respect to time such that time zero represents the 30-second record during which the first modified opening was observed, and time = 1.0 represents the first 30-second record during which all openings were of modified conductance. Symbols are mean ± SEM for each time-point; solid line represents fit to an exponential function. This normalization takes into account the variable diffusion rate in each experiment, due to variation in the tip diameter and volumes of $MTSET^+$-free and $MTSET^+$-containing pipette solution.

A potential confounding factor in the analysis of the time-course of current changes due to single or multiple exposures to $MTSET^+$ is the possibility that during the exposure to $MTSET^+$ the number of active channels was changing. We analyzed single-channel recordings containing multiple R334C-CFTR channels in excised mode, while $MTSET^+$ diffused down to the tip from a backfilled pipette; the example shown in Fig. 14 contained at least three active channels. The sample traces (Fig. 14A) represent the 30-second spans near the beginning of the experiment, near the middle, and near the end of the experiment, such that the first modified channel opening (indicated by a green bar) is shown in the first trace and all openings in the third trace are already modified. One can see that the single channel amplitude of the last modified opening is almost identical to that of the first modified opening. We counted the number of modified and unmodified openings within successive 30-second windows, and plotted the number of unmodified openings (open circles) and modified openings (closed circles) as a function of time (Fig. 14B). As $MTSET^+$ diffused down the pipette, more channel openings exhibited the modified conductance, and fewer exhibited the unmodified conductance. This confirms that the modified openings with higher conductance arose from the same channels as the unmodified openings with low conductance, and were not due to the $MTSET^+$-induced appearance of other channels in the patch. To account for changes in channel number due to rundown during the long recording, we plotted the fraction of all openings per segment that exhibited the modified conductance as a function of time (Fig. 14C). The concentration of $MTSET^+$ at the membrane surface should increase through time in an exponential fashion by diffusion. Fig. 14C shows that the fraction of openings that exhibited the modified conductance in each 30-second segment also increased with time in an exponential fashion. This was true for the single experiment shown in Fig. 14C and for five other multichannel patches, where the time to reach complete modification was normalized in order to account for differences in tip diameter and backfill volume (Fig. 14D). These results strongly argue that the process of the $MTSET^+$-induced increase in current reflects modification of existing channels at the surface of the membrane.

4.2. To determine how binding and hydrolysis of ATP at the NBDs controls the conformation of the pore

4.2.1. R334C channels are modified by MTSET$^+$ only in the closed state

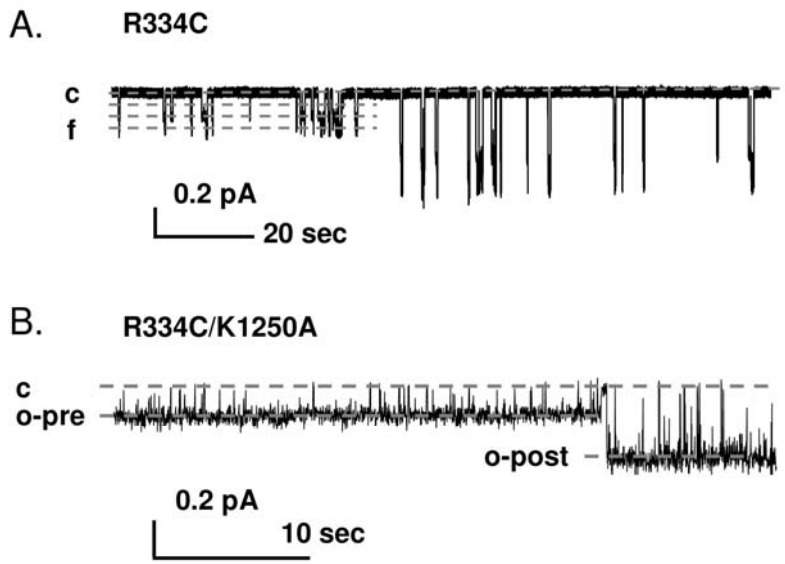

Fig.15. **Real-time modification of R334C-CFTR and R334C/K1250A-CFTR channels by MTSET$^+$. (A)** A representative trace for R334C-CFTR in the excised, inside-out patch configuration during real-time modification by MTSET$^+$ back-filled in the pipette. Over the course of 10-15 min, the channel was modified by MTSET$^+$ diffusing into the tip of the patch pipette, as reflected by the increase in the single-channel amplitude. Modification occurred between the end of the last unmodified opening with lower amplitude, and the beginning of the first modified opening with higher amplitude, *i.e.*, while the channel was closed. Current levels for unmodified R334C-CFTR are indicated by the four dashed lines (in order from the top to bottom): **c**, **s1**, **s2** and f represent the closed, subconductance 1, subconductance 2 and full conductance states. **(B)** Representative trace for R334C/K1250A-CFTR under identical conditions. Current levels are indicated by dashed lines: c, o-pre and o-post represent the closed, unmodified-open, and modified-open, respectively.

We have previously shown that the MTSET$^+$-induced covalent modification of a cysteine engineered at CFTR's position 334 (in TM6) increased single-channel conductance without altering gating properties (Fig. 5) [79]. In contrast, WT-CFTR does not respond to either MTSET$^+$ or MTSES$^-$ when these reagents are applied to the

outside surface of the membrane (Fig. 5) [79]. Excised, inside-out patch clamp recordings in which the pipette was backfilled with $MTSET^+$ allowed us to watch the process of modification in real-time as the $MTSET^+$ diffused to the electrode tip and deposited positive charge at the engineered cysteine (Fig. 15A). Despite hours of recording of R334C-CFTR channels, the process of modification was observed to occur only during the closed interval (*i.e.*, sometime between the last opening with lower conductance and the first opening with higher conductance). This observation led us to hypothesize that modification of R334C-CFTR might be favored by the closed state. To test this hypothesis, we coupled the R334C mutation with a mutation at the Walker lysine of NBD2, K1250A, which prolongs the open burst duration of CFTR channels [34; 38; 157]. Figure 15B shows a recording of a single R334C/K1250A-CFTR channel, where the electrode was backfilled with 200 μM $MTSET^+$. Modification was delayed until the channel transitioned to a brief closed state. Upon re-opening, channel amplitude was increased, reflecting covalent modification by $MTSET^+$. Hence, even when P_O was increased by the K1250A mutation, modification at R334C did not take place in the open state. These observations strongly suggest that modification of R334C-CFTR by $MTSET^+$ is favored by the closed state.

As shown in Figures 7B, 8A, 9A, 9B and 15A, and reported previously [17], R334C-CFTR channels exhibit stable subconductance behavior, including transitions to **s1**, **s2**, and **f** conductance states. In contrast, all of the open bursts of R334C/K1250A-CFTR before modification lacked transitions between conductance states and were "locked" in the **s2** state (Fig. 15B). Following $MTSET^+$-induced modification, R334C/K1250A-CFTR channels opened to, and remained locked in, the **s2** state. Amplitudes for the **s2** state in R334C/K1250A-CFTR were not significantly different from the amplitudes of the **s2** state of R334C-CFTR before and after modification ($p = 0.85$). These data suggest that interruption of the ATP-dependent gating cycle leads to stabilization of the pore conformation, resulting in fewer transitions between the three open conductance levels characteristic of R334C-CFTR; this provides further support for the notion that transitions between open conductance levels in CFTR channels are linked to NBD-mediated gating events.

4.2.2. Macroscopic kinetics of modification were altered in the presence of AMP-PNP

If modification of R334C-CFTR is favored by the closed state, we would expect to observe a slowing of the macroscopic time course of modification under conditions that increase P_O. To test this hypothesis, we studied outside-out macropatches pulled from oocytes expressing R334C-CFTR. Following steady state activation by ATP and PKA in the pipette, the outside surface of the membrane was rapidly exposed to a solution containing 10 μM $MTSET^+$. Under standard conditions, where the pipette solution contained ATP, rapid exposure to $MTSET^+$ caused an increase in macroscopic current (Fig. 16A); the time-course of modification in all four experiments of this type was best described by a first-order exponential, with time constant $\tau = 5.93 \pm 1.37$ sec (Table 2).

We converted the time-constant to a modification rate coefficient as described in Experimental Procedures, giving a value of 18,922 ± 3,218 $M^{-1}s^{-1}$. To increase the P_O of R334C-CFTR channels, we included a poorly hydrolyzable ATP analogue, AMP-PNP, at 2.75 mM in addition to ATP in the pipette [158; 159]. Figure 16B shows that the increase in macroscopic current upon exposure of R334C-CFTR channels to $MTSET^+$ in the presence of cytosolic ATP + AMP-PNP exhibited a somewhat different time-course compared to experiments with ATP alone. Although we expected a much slower modification process, the kinetics of modification in the presence of AMP-PNP were fit best with the sum of two exponential functions, with time constants $\tau_1 = 4.35 \pm 0.9$ sec (fractional amplitude: 69 ± 4%) and $\tau_2 = 157 \pm 14.9$ sec (fractional amplitude: 31 ± 4%; Table 2). The modification rate coefficients were 20,636 ± 4,984 $M^{-1}s^{-1}$, and 684 ± 93 $M^{-1}s^{-1}$, respectively. Hence, modification of R334C-CFTR in the presence of mixtures of ATP and AMP-PNP occurred in two phases. The value of the time-constant describing the faster phase of modification in the presence of AMP-PNP (τ_1) was not statistically different from the single time-constant (τ) in the presence of ATP alone ($p = 0.362$), nor were the modification rate coefficients different ($p = 0.286$). WT-CFTR channels in the presence of mixtures of ATP and AMP-PNP alternate between openings of normal duration, when ATP is bound at both NBDs, and prolonged openings, when

AMP-PNP is bound at NBD2 [105; 106]. The slower phase of macroscopic modification in the presence of AMP-PNP may reflect the process of modification of those channels that are locked into a long open burst. The faster phase of modification in the presence of AMP-PNP may reflect the modification process of channels exhibiting open bursts of normal duration.

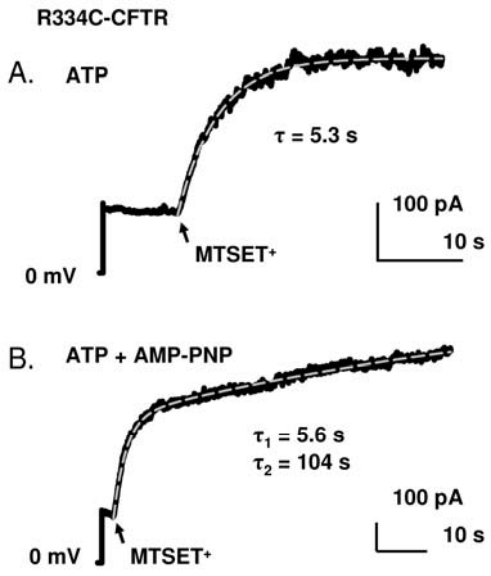

Fig.16. **Modification of R334C-CFTR is slowed in the presence of AMP-PNP.** **(A)** A representative recording of macroscopic current of R334C-CFTR. The pipette potential was held at 0 mV, and then stepped to +80 mV. The arrow indicates the rapid application of 10 μM $MTSET^+$ to the outside surface of the patch. The dashed line indicates a fit of the data to a first-order exponential function with $\tau = 5.3$ sec in this record. **(B)** A representative recording of macroscopic current from R334C-CFTR in the presence of ATP + AMP-PNP. The kinetics of modification under this experimental condition were described best by the sum of two exponential functions, with values of $\tau_1 = 5.6$ sec and $\tau_2 = 104$ sec in this record.

To understand better the results from macropatch experiments, we performed detached inside-out single-channel recordings in R334C-CFTR, in the presence of ATP + AMP-PNP, using the real-time modification approach. In Figure 17, three traces shown are from the same patch containing at least 3 active channels; traces A, B, and C are from near the beginning, near the middle, and near the end of the experiment, respectively. One can clearly see that there are two populations of open bursts which differ in duration: the vast majority of openings are brief, such as those seen in the absence of AMP-PNP; other prolonged openings arise from channels that are locked open (arrow in trace A). During real-time modification by $MTSET^+$, channel openings increased in amplitude, but with different time-courses. All modified openings in the

middle trace were brief ones, while the prolonged openings remained unmodified, and all openings in the third trace were already modified. On average, the first modified prolonged opening appeared 147.6 ± 43.2 sec later than the first modified brief opening; in five out of six patches *all* brief openings were modified before the first prolonged one was modified. Furthermore, the prolonged unmodified openings and prolonged modified openings induced by AMP-PNP were "locked" in the **s2** state, as was found for R334C/K1250A-CFTR with ATP alone, and the **s2** state amplitudes were virtually identical to those for the **s2** state of R334C-CFTR in the presence of ATP alone ($p > 0.5$).

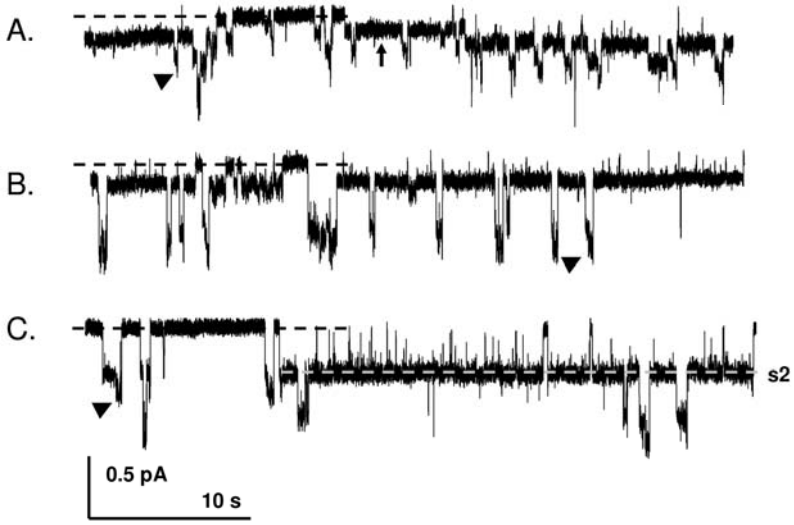

Fig.17. **Real-time modification of R334C-CFTR in the presence of ATP + AMP-PNP.** Three traces from one single-channel patch recording in excised, inside-out mode, with real-time modification by diffusion of $MTSET^+$ to the patch tip. This individual patch contained at least three active R334C-CFTR channels, recorded in the presence of ATP +AMP-PNP. Experimental conditions were otherwise identical to those in Figure 15. **(A)** The first trace, from early in the experiment, shows two channels locked open (up arrow indicates an example of a locked-open burst) and at least one undergoing normal gating (arrowhead). Neither is modified. **(B)** In the second trace, from near the middle of the experiment, only the channel that was not locked open has undergone modification. **(C)** In the third trace, later in the record, both channels have been modified, but only one is locked open. Arrowheads indicate the **s2**-to-**f** transition in unlocked channels, for an unmodified channel in the upper trace and for modified channels in the middle and lower traces. The lower dashed line in the bottom trace shows that channels locked open by AMP-PNP were locked into the **s2** open state (compare to the unlocked opening at left). The upper dashed lines represent the closed current level.

The data in Fig. 17 showed the similar results as observed by Carson *et al*. in WT-CFTR [38], that additional AMP-PNP triggers a new single channel state (the locked-open state) into the gating scheme, making them less reactive toward $MTSET^+$; this would lead to the appearance of a slow component in the modification rate coefficient, therefore, data was described best by the sum of two exponential functions (Fig. 16). Hence, these results suggest that the modification rate coefficient slows under conditions that increase P_O, which is consistent with the notion that $MTSET^+$-induced modification in R334C-CFTR is favored by the closed state.

4.2.3. Kinetics of macroscopic modification were altered in NBD mutants

As described above, CFTR channel P_O can be altered by mutations at the Walker A lysines that are involved in catalysis of ATP [34; 38; 157]. Mutation K1250A reduces channel closing rate (Fig. 15B). Mutation K464A in NBD1 leads to a great reduction in channel opening rate. We studied outside-out macropatches from oocytes expressing R334C/K1250A- or R334C/K464A-CFTR to determine the effects of these gating domain mutations on the kinetics of modification, using experimental procedures similar to those described above. Upon exposure to $MTSET^+$, the macroscopic current for R334C/K1250A-CFTR increased rapidly at first, followed by a slower increase in current, reflecting a complicated modification process (Fig. 18A); the kinetics of modification were described best by the sum of two exponential functions. Hence, the consequences of introducing the K1250A mutation were similar to the consequences of addition of non-hydrolyzable nucleotide: the time-course of macroscopic modification was biphasic, with a component that is much slower than that seen in the single mutant with ATP alone. In five experiments (Table 2), τ_1 averaged 12.5 ± 0.94 sec (fractional amplitude: 74.7 ± 1.3%), which was significantly larger than the value of τ for R334C-CFTR in the presence of ATP alone and the value of τ_1 for R334C-CFTR in the presence of ATP + AMP-PNP ($p<0.001$). For those five experiments, τ_2 averaged 225 ± 29 sec (fractional amplitude: 25.3 ± 1.3%), which was somewhat larger than the value of τ_2 for R334C-CFTR in the presence of ATP + AMP-PNP ($p = 0.049$). The modification rate coefficients for $MTSET^+$ in R334C/K1250A-CFTR were 9,840 ± 626

$M^{-1}s^{-1}$ and 482 ± 65 $M^{-1}s^{-1}$, respectively.

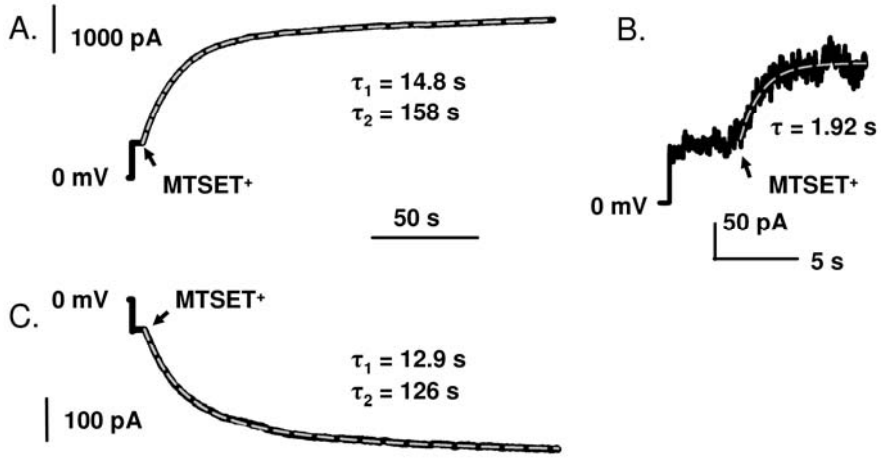

Fig.18. **$MTSET^+$-induced modification of R334C/K1250A-CFTR and R334C/K464A-CFTR.** Outside-out macropatches from oocytes expressing either R334C/K1250A-CFTR (**A** and **C**) or R334C/K464A-CFTR (**B**). Experimental conditions were identical to those in Fig.16. The pipette potential was held at 0 mV, and then stepped to either +80 mV (**A** and **B**) or -80 mV (**C**). The arrows indicate the rapid application of 10 μM $MTSET^+$. The process of modification of R334C/K1250A-CFTR by $MTSET^+$ at V_M = +80 mV was fit best with the sum of two exponential functions, with τ_1 = 14.8 sec and τ_2 = 158 sec in this experiment. The kinetics of modification of R334C/K1250A-CFTR by $MTSET^+$ at V_M = -80 mV also were described best by the sum of two exponential functions, having values of τ_1 = 12.9 sec and τ_2 = 126 sec in this experiment. In contrast, the kinetics of modification of R334C/K464A-CFTR by $MTSET^+$ were fit best with a first-order exponential function, with τ = 1.92 sec in this experiment.

The biphasic nature of the macroscopic kinetics of modification in these experiments likely reflects the fact that the K1250A mutation reduces the closing rate in some channels but not all [157]. In other words, while R334C/K1250A-CFTR channels are closed, they stay closed approximately as long as R334C-CFTR channels do, which provides an opportunity for rapid modification. When R334C/K1250A-CFTR channels are open, they typically stay open much longer than R334C-CFTR channels do, which reduces the macroscopic modification rate coefficient [129]. In a manner similar to the experiments using R334C-CFTR in the presence of ATP + AMP-PNP, the briefer open bursts were always modified earlier than the longer bursts (data not shown).

We also reasoned that if modification of R334C-CFTR channels is favored by the closed state, the modification rate coefficient should be higher under conditions that reduce P_O. To test this hypothesis, we first studied outside-out macropatches of R334C-CFTR channels in the presence of 0.2 mM ATP and measured the kinetics of modification. Surprisingly, the time constant of modification was identical to that observed for R334C-CFTR in the presence of 1 mM ATP ($p = 0.72$; Table 2). We speculated that 0.2 mM ATP may slightly reduce the P_O of R334C-CFTR channels, but not to a degree that could alter significantly the kinetics of modification; indeed, the overall P_O of R334C-CFTR channels recorded in the presence of 1 mM ATP is already reduced, compared to WT-CFTR under identical conditions (0.24 ± 0.04 (Fig. 8E) *vs.* 0.34 ± 0.03 (Ref 107), respectively). Therefore, we recorded from giant outside-out patches pulled from oocytes expressing R334C/K464A-CFTR, which would reduce P_O considerably by prolonging the interburst closed durations [24; 38; 157] (Fig. 18B). The macroscopic current of R334C/K464A-CFTR was increased rapidly upon application of 10 μM $MTSET^+$. The kinetics of modification were described best by a first-order exponential (Table 2; $p = 0.004$ compared to τ for R334C-CFTR). The modification rate coefficient for $MTSET^+$ in R334C/K464A-CFTR was 41,864 ± 4,229 $M^{-1}s^{-1}$, which is roughly 2-fold higher than that in R334C-CFTR under identical conditions ($p = 0.007$). Hence, the prolonged interburst closed duration led to an increase in modification rate coefficient.

4.2.4. Kinetics of modification by $MTSES^-$

Because our previous studies (Fig. 11) [79] showed that the electrostatic potential in the outer vestibule affects the kinetics of modification at R334C, we asked whether the modification rate coefficient (and its potential state-dependence) for a negatively charged SH-modifying reagent was different from that measured for the positively charged $MTSET^+$. Figure 19 shows outside-out macropatch recordings from oocytes expressing either R334C-CFTR or R334C/K1250A-CFTR, with rapid exposure to 50 μM $MTSES^-$. Macroscopic currents from R334C- and R334C/K1250A-CFTR were decreased upon exposure to $MTSES^-$ (due to deposition of negative charge) by 75

± 6% and 77 ± 5%, respectively. The kinetics of modification of R334C-CFTR by $MTSES^-$ were fit best with a first-order exponential function (Table 2). The macroscopic kinetics of modification of R334C/K1250A-CFTR were fit best with the sum of two exponential functions (Table 2; the fractional amplitudes were 84 ± 2.7% for τ_1 and 16 ± 2.7% for τ_2), as was found for $MTSET^+$. The modification rate coefficients for $MTSES^-$ in both R334C-CFTR and R334C/K1250A-CFTR were >3-fold lower than those measured for $MTSET^+$ in the same mutants ($p < 0.001$). These results suggest that electrostatic profiles may influence the rate of modification by SH-modifying reagents. More importantly, the kinetics of modification of the engineered cysteine at R334C by $MTSES^-$ were state dependent, as described above for modification by $MTSET^+$.

Because one might suggest that the apparent state-dependence of modification reflects interference from Cl^- in or near the mouth of the channel, we next asked whether the direction of Cl^- movement affected the kinetics of modification by extracellular $MTSET^+$. Figure 18C shows a representative experiment, where V_M was held at 0 mV and then stepped to -80 mV. Upon rapid exposure to $MTSET^+$, macroscopic inward current was increased reflecting modification of R334C/K1250A-CFTR channels. The kinetics were fit best with a sum of two exponential functions, providing time-constants that were very similar to those measured from experiments at V_M = +80 mV (τ_1 = 13.4 ± 0.8 sec and τ_2 = 217 ± 52 sec; n = 3; $p > 0.5$). These results indicate that the direction of anion movement does not affect the rate of modification by SH-modifying reagent at R334C.

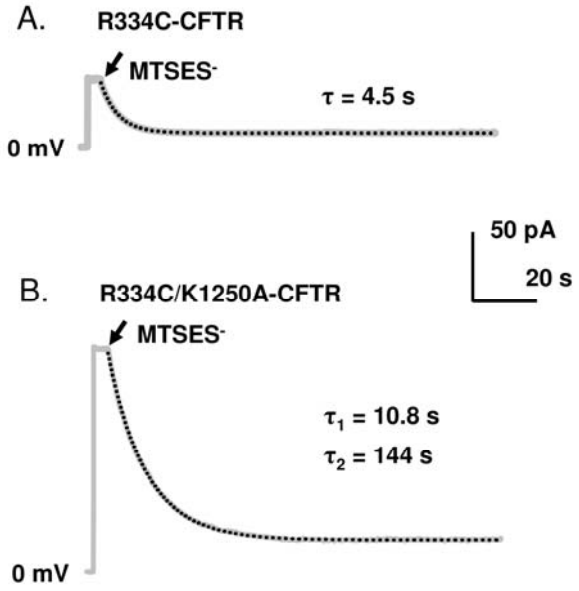

Fig.19. **MTSES$^-$-induced modification of R334C-CFTR and R334C/K1250A-CFTR.** Outside-out macropatches were pulled from oocytes expressing either R334C-CFTR or R334C/K1250A-CFTR. Experimental conditions were similar to those described in Figures 16 and 19. (**A**) R334C-CFTR channels were activated by ATP + PKA. The amplitude of macroscopic current was decreased by 79% upon modification by 50 μM MTSES$^-$ in this experiment. The dashed line indicates a fit of the data to a first-order exponential function, having $\tau = 4.5$ sec in this experiment. **(B)** A representative recording of macroscopic current of R334C/K1250A-CFTR under identical conditions. The process of modification in the double mutant was fit best by the sum of two exponential functions (dashed line), with values of $\tau_1 = 10.8$ sec and $\tau_2 = 144$ sec, respectively, in this experiment. The amplitude of macroscopic current was decreased by 85% upon modification by MTSES$^-$.

Table 2. Kinetics of modification of R334C under a variety of conditions.

Condition	1 mM ATP	0.2 mM ATP	1 mM ATP	1 mM ATP + 2.75 mM AMP-PNP	1 mM ATP	1 mM ATP	1 mM ATP	1 mM ATP
Mutant	R334C	R334C	R334C/K464A	R334C	R334C/K1250A	R334C	R334C	R334C/K1250A
[$MTSET^+$]	10 µM	10 µM	10 µM	10 µM	10 µM	50 µM		
[$MTSES^-$]							50 µM	50 µM
τ in seconds (n)	5.93 ± 1.37 (4)	5.88 ± 0.49 (5)	2.44 ± 0.27 (3) *	4.35 ± 0.9 and 157 ± 14.9 (5)	12.5 ± 0.94 and 225 ± 29 (5) *	2.73 ± 0.24 # (5)	4.23 ± 0.18 (3) ¶	11.3 ± 0.7 and 132 ± 30.1 (5)

Values given are mean ± SEM.

*, significant difference from value for R334C-CFTR with 1 mM ATP, exposed to 10 µM $MTSET^+$.

¶, significant difference from value for R334C-CFTR with 1 mM ATP, exposed to 50 µM $MTSET^+$.

#, significant difference from value for R334C-CFTR with 1 mM ATP, exposed to 50 µM $MTSET^+$.

5. Discussion

5.1. Anion conduction by CFTR: One pore per polypeptide

The results presented here are compatible with the hypothesis that a single, 170 kDa CFTR polypeptide forms a single, anion-selective conduction pathway in the functional protein (Fig. 20A). Previous studies of the channel function of CFTR, including its substate behavior, have been interpreted in terms of two other, rather disparate conduction models [160]. In one, proposed by Guggino and coworkers [65; 136; *see also* 66] a single CFTR polypeptide can form two pores (one from MSD1 and another from MSD2) while in the other, proposed by several investigators [60; 61; 161; 162] the formation of a single pore requires the association of two CFTR monomers. Evidence supporting the one-polypeptide, two-pore model was derived from studies of channel activity recorded from cells that were induced to express fragments of the parent CFTR polypeptide. For example, Guggino and coworkers [136] reported that full-length WT-CFTR exhibited two subconductance levels that summed to the full conductance level. Channels formed from constructs expressing only the front half of CFTR or only the back half of CFTR exhibited different conduction and gating properties; the properties of channels from CFTR's front half were more like those of WT channels. These studies, while intriguing, suffer from several limitations. First, the observation of channel activity that could be attributed to a CFTR fragment would not necessarily imply that the same fragment would form a similar conducting structure when it resided within the parent molecule. Second, it is difficult to unequivocally attach a particular observed channel activity to a particular fragment without mutagenesis or covalent labeling studies; two copies of the front half [55], or two copies of the back half [163], might dimerize to form channels that have no relation to the activity of the intact protein. Finally, there is disagreement as to whether CFTR fragments actually produce channel activity [164].

Evidence for the one-pore, two-polypeptide model was derived from studies of channel function detected in cells expressing CFTR concatemers comprising two polypeptides expressed in tandem. Ma and coworkers [60, 61] reported that the gating properties of channels formed from such constructs were intermediate between

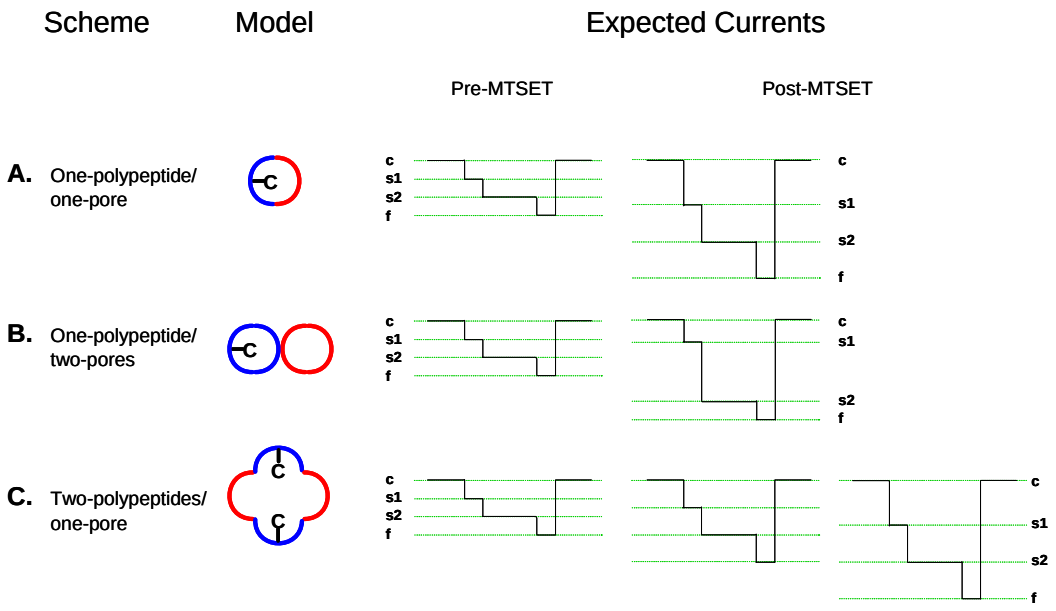

Fig. 20. **Three proposed schemes for the structure of the minimum functional unit for the CFTR channel.** Models show pores built from combinations of domains from the front-half of the CFTR polypeptide (blue) and the back-half of the CFTR polypeptide (red). The engineered cysteine residue is shown at the extracellular end of TM6. The expected currents are shown schematically for channels before and after modification by $MTSET^+$.

those seen when either of the two polypeptides was expressed individually, but that these channels opened to a single level with the same conductance as channels expressed individually. These results are provocative, but do not rule out the possibility that the observed channel behavior can be attributed to activity of one of the two monomers, modified in some way by forced association with a partner. Low resolution structures of CFTR were interpreted as suggesting that two CFTR polypeptides can dimerize in plasma membranes [62; 165] but these images do not make any predictions as to whether these putative dimeric structures comprise one pore or two. In contrast, recent structural data from electron microscopy was interpreted as suggesting that CFTR resides in the membrane as a monomer [71]. Moreover, we never observed that two steps of modification by $MTSET^+$ occurred as illustrated in Fig. 20C despite many hours of recording.

In the present experiments we compared the subconductance behavior of wild type and mutant CFTRs and investigated the effect on subconductance behavior of covalent charge deposition using R334C-CFTR. There was a remarkable consistency in the subconductance behavior among the various CFTR constructs, each exhibiting three conductance amplitudes approximately in the ratio of 1: 1.4 : 2.1, but with distinctly different kinetics. In patches from cells expressing R334C-CFTR the substate amplitudes were simultaneously increased in nearly identical proportion upon modification by $MTSET^+$. This result is significant for two reasons. First it demonstrates unequivocally that the subconductance states reported here are, in fact, a property of the CFTR channel. Second, this result strongly suggests that all three conducting conformations share at least a portion of the same conduction path, that which contains the arginine at position 334. This finding is not compatible with the notion that subconductance states represent the properties of two, completely separate conduction pathways formed, for example, by MSD1 or MSD2, respectively. Rather, the present results support a model in which the subconductance pathways utilize at least a common outer vestibule that contains R334.

It is also difficult to reconcile the results presented here with any model requiring the anion-conducting pore to be formed at the interface between two CFTR monomers (Fig. 20C), in the manner analogous to the structure now well-established for potassium-selective channels [166]. In the simplest conception of such a model, as proposed by Zerhusen et al. [61], a dimeric pore would be expected to contain two copies of R334 (or C334). Neither the impact of covalent labeling nor the kinetics of labeling provided any evidence for the presence of more than a single cysteine in the pore formed by R334C-CFTR. In the absence of a crystal structure we cannot eliminate the hypothesis that a dimeric conducting pore is formed in such a way as to render the location and functional significance of the R (or C) at 334 highly asymmetric, as in some sort of "head-to-tail" conformation, but this would require some major contortions of the protein topology if the true structure of CFTR resembles in any way that of other ABC superfamily proteins.

These conclusions rely on the assumption that R334 lies within the pore or within the outer vestibule. We have previously provided evidence that is consistent with a model for the conduction path in which R334 lies within the vestibule of the pore where it functions to increase the local concentration of permeant anions [79]. This evidence is based on essentially two findings. First, functional modification of R334C CFTR by reagents such as $MTSET^+$ and $MTSES^-$ indicates that a cysteine at position 334 lies within the outward facing, water-accessible surface of the protein. Second, a detailed examination of the nature of the functional modification of R334C, particularly with regard to the impact of $MTSET^+$, was consistent with the effects of a vestibule charge. The functional effects are strictly charge-dependent, whether brought about by covalent modification or pH titration of the engineered cysteine. We have shown that even the effects of a neutral compound like NEM can be understood in terms of the charge that is neutralized in the formation of the thioether bond. Furthermore, for $MTSET^+$, we have shown that single-channel conductance is increased and that, in three separate sets of experiments, there is no discernable change in P_O when R334C is modified. Finally, we have shown that the change in macroscopic conductance and I-V or i-V shape can be described by a simplified model incorporating a charged vestibule in which only the outer vestibule electrostatic potential changes after modification [79]. Others have also suggested that R334 provides fixed positive charge in the outer mouth of the pore that plays a role in anion permeation [167]. While these findings do not allow us to unequivocally place R334 in the outer vestibule of the CFTR pore, it seems quite appropriate to conclude that the available evidence is consistent with a model that places R334 in the pore.

The simplest interpretation of the results presented here is that a single CFTR polypeptide folds in such a way as to form a single, anion-conducting pore (Fig. 20A). Several laboratories have attempted to identify the structure of the pore of CFTR by examining the behavior of CFTR protein isolated and detergent solubilized using a variety of methods, but these studies have not produced entirely consistent results [160]. Using chemical cross-lining and non-dissociative polyacrylamide gel electrophoresis, Bear and coworkers [168] studied the quaternary structure of purified, reconstituted CFTR, and suggested that CFTR exists in monomeric form, which gated to a single

open level in planar lipid bilayers, but that reconstitution of CFTR monomers often led to formation of dimers. Chen et al. [160] reported the results of biochemical and biophysical studies of CFTR and could find no evidence of hybrid channels when WT-CFTR was co-expressed with either of several pore-domain mutants. Several recent studies reported that two CFTR molecules indeed may be induced to interact through binding of scaffolding proteins containing bivalent or multivalent PDZ domains, such as CAP70 [161] and NHERF [162], which appeared to result in an increase in the activity of a single pore, rather than an increase in the number of open levels. However, it is not clear that the MSDs from both of the interacting CFTR peptides were contributing to chloride permeation. Further, because channels were evident in the record before addition of the PDZ peptides, it is apparent that the formation of the minimum functional unit does not require PDZ-mediated interactions between multiple CFTR peptides.

CFTR is a member of the large ABC Transporter superfamily of proteins, which has been studied extensively. Rosenberg et al. [169] reported that lectin-gold labeling of the single glycosylation site in P-glycoprotein resulted in particle size that was consistent with the monomeric form. In the same system, which is highly homologous to CFTR, Loo and Clarke [170, 171] used site-directed mutagenesis to study the substrate-binding pocket; TM domains in both the front and back halves of the full-length P-glycoprotein peptide contribute to the substrate-binding pocket, and may be crosslinked to each other by aqueous reagents. Finally, the structures of two *E. coli* ABC Transporters, MsbA and BtuCD, were recently solved to 3.7 and 3.2Å, respectively [98, 172]. The crystal structures of these half-transporters, encoding one MSD and one NBD per peptide, clearly show that two half-transporters dimerize to form the functional proteins, with one substrate-binding pocket (not two) formed from TM helices from each of the two MSDs (not four). By analogy, these structures suggest that the single substrate-binding pocket (or pore) of full-length CFTR may be comprised of TM domains from both MSDs in a single CFTR peptide.

5.2. Subconductance states: Implications for channel structure and function

WT-CFTR channels exhibit infrequent transitions to one or more subconductance levels, which appear to have properties, such as susceptibility to pore blockers (see below) that differ from that of the full conductance level [76; 86; 138]. The behavior of the subconductance states seen in the CFTR constructs reported here raises questions about the structural basis for the observed conductance levels. The relative amplitudes and the shared responses to covalent labeling in R334C-CFTR suggest two potential models, diagrammed in Fig. 21. In model A, two relatively separate channels empty into a common, outer vestibule. In this scheme the two lower conductance states would represent the properties of either the left-hand or right-hand channel alone and the full conductance state their approximate sum. In model B a single pore that empties into the outer vestibule can assume three, distinct conducting conformations. Although the present data alone cannot distinguish between these two possibilities, the single-pore model (B), taken in the context of the structure of CFTR's ABC Transporter relatives, seems the most parsimonious.

It is important to point out that the results reported here do not eliminate the possibility that yet additional conducting conformations exist, resulting in additional subconductance levels, which could not be discerned here because of the recording conditions utilized. Also, an important caveat in the present study is that most of these results rely upon experiments using CFTR mutants; these mutants clearly altered the structure of the pore, at least to the extent that the electrostatic potential in the outer mouth of the pore was changed [79]. However, these channels retained chloride selectivity and dependence upon PKA + MgATP, suggesting that gross changes in channel structure did not occur. Our interpretation of the results in this study rests on the assumption that these single-site or dual-site cysteine mutations in the pore domain did not alter the fundamental structure of the functional CFTR channels.

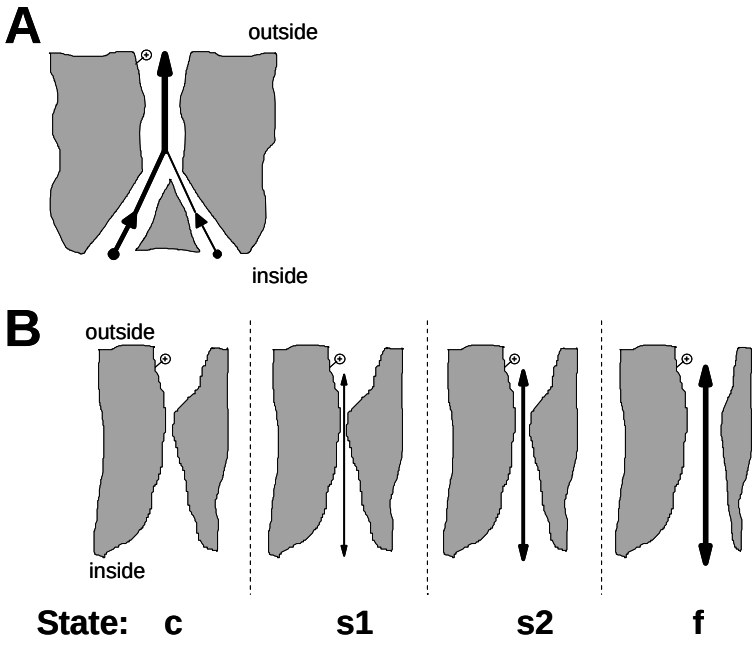

Fig.21. **Two distinct models for the composition of the permeation pathway in CFTR, based on the results of this study**. In **(A)**, two pathways diverge at the cytoplasmic end of the channel, but share a common conduction pathway at the extracellular end. The **s1** and **s2** states would reflect conduction through the right and left pathways, respectively, while the **f** state would represent the simultaneous conduction through both pathways. In **(B)**, a single pathway is formed from extracellular to cytoplasmic ends of the pore. We speculate that conformational changes in the pore, resulting in the four stable configurations shown, result in different rates of permeation.

Subconductance states are common in many types of ion channels, and may arise from permeation through distinct pores, as in the ClC voltage-gated Cl^- channels [173-176] or alternative conformations of a single pore, as in voltage-gated K^+ channels [177]. Several pieces of evidence suggest that the CFTR pore exhibits more than two conformations (open and closed). For instance, the different conductance states exhibit different pharmacology: the subconductance states of WT-CFTR appear to be less susceptible to block by DPC than is the full conductance state [76; 86]. It is not yet known whether the three conductance states exhibit differences in anion selectivity [*but see* 136].

The observations of Ishihara and Welsh [138] suggested that CFTR single channels can reside in two different open states: one that is susceptible to block by the pH buffer MOPS from the intracellular solution (O1 state), and one that is not (O2 state); in these studies the conductance of O1 was ~80% that of O2. Furthermore, the occupancy of those states was not random, since the MOPS-insensitive O2 state was almost always visited at the end of an open-channel burst, leading to an apparent increase in single-channel conductance due to relief from fast pore block. (Interestingly, R334C-CFTR channel openings also appear to be nonrandom in the order of sojourns in the three conductance states, as they transition to the full conductance state at the end of most bursts [Fig. 7, 8, and 9]. The addition of non-hydrolyzable ATP analogs prevented the transition from the O1 (equal to **s2**) state to the O2 (equal to **f**) state, suggesting that ATP hydrolysis alters the conformation of the pore [138]. Other investigators have reported that subconductance states were visited more frequently in channels bearing deletions in one of the intracellular loops connecting TM domains, suggesting that these loops may interact with the NBDs to stabilize the open state [142; 143].

CFTR channels are permeable to large anions such as gluconate from the intracellular solution but not from the extracellular solution; this asymmetry is dependent upon ATP hydrolysis, since inhibitors of hydrolysis allow extracellular gluconate to permeate [149]. These results suggest that the pore may exist in multiple conformations, with different selectivity characteristics, determined by the activity of the nucleotide-binding folds. Voltage-dependent behavior of CFTR channels can be induced by the V317E mutation, in TM5, and by the S1118F mutation, in TM11, resulting in voltage-jump relaxations of macroscopic currents [144; 145]; WT-CFTR shows no such behavior. In the case of S1118F-CFTR, the selectivity of the channel pore changes during these relaxations, and the rate of the relaxation depends upon the character of the permeating anion [144]. This suggests that the same TM segments that confer CFTR's permeation properties may also contribute to gating its pore. In this regard, it is important to note that amino acid substitutions in the TMs can influence gating by altering the prevalence of a particular substate.

Taken together, the results in this study are consistent with the notion that the functional CFTR channel is built following the one-polypeptide/one-pore model; further experiments will be required to distinguish between the two models of Fig. 21. While there remains a possibility that multiple CFTR polypeptides may dimerize in epithelial cells, perhaps due to interaction with PDZ-domain proteins, each of these CFTR polypeptides would be expected to comprise a separate pore.

5.3. Changes in the conformation of the outer vestibule of the CFTR channel pore between open and closed states.

In the second objective of the thesis study, we made use of covalent modification of engineered cysteine residues to investigate potential changes in the conformation of the outer vestibule of the CFTR channel pore between open and closed states. Single R334C-CFTR channels studied using real-time modification only showed a reaction to $MTSET^+$ during a closed state, even when channel P_O was increased dramatically by exposure to mixtures of ATP and AMP-PNP, or by addition of the Walker A mutation K1250A. Macropatch currents recorded from oocytes expressing R334C-CFTR increased rapidly upon abrupt exposure to $MTSET^+$ (or decreased rapidly upon abrupt exposure to $MTSES^-$). Under conditions that increase channel activity (*i.e.*, R334C-CFTR with ATP + AMP-PNP, or R334C/K1250A-CFTR with ATP alone), the kinetics of modification were slowed. Under conditions that decrease channel activity (R334C/K464A-CFTR), the rate of modification was increased dramatically. These data are consistent with a difference in the reactivity of the engineered cysteine to SH-modifying reagents between the open and closed channel states which most likely reflects changes in the conformation of the pore, or at least the outer vestibule, driven by gating events at the NBDs. These results provide the first evidence of movement in the CFTR pore domain correlated with channel gating state.

Our data indicate that the rate of covalent modification at R334C differs dramatically between closed and open channels. This result could be explained by physical hindrance of the interaction between the reagent and the cysteine if the side

chain were buried in protein or lipid during the open state. However, we previously found that the macroscopic conductance of whole oocytes expressing R334C-CFTR channels was sensitive to bath pH, due to titration of the partial negative charge on the unmodified cysteine (Fig. 13) [79]. This observation suggests that R334C indeed faces the water soluble pore while the channels are open because protons can access this residue. Hence, the state-dependent ability of MTS reagents to interact with the engineered cysteine of R334C-CFTR most likely reflects a difference in the reactivity of that cysteine during channel closure, rather than physical obstruction that reduces accessibility. The difference in reactivity may reflect the impact of another residue, which shifts the pKa for $MTSET^+$. Hence, we cannot say that R334C changes its position between open and closed states, but rather must limit ourselves to saying that the orientation of R334C relative to the other residue, or the distance between them, changes as a function of channel gating. Nonetheless, these data suggest that changes in the rate coefficients for SH-modifying reagents at R334C under different experimental conditions reflect conformational changes in the outer vestibule of the CFTR pore, which are associated with ATP-dependent gating.

Our results also provide further evidence that transitions between the three major open conductance states are linked to ATP-dependent gating events at the NBDs. As described previously [79], channels formed by WT-CFTR, and many pore-domain mutants, including R334C-CFTR, exhibit two subconductance states (**s1** and **s2**) as well as the full conductance state (**f**) (Figures 7, 8 and 9). The subconductance states in some mutant channels differ markedly in their stability and probability of occurrence from that seen in WT-CFTR (Fig. 7). Interestingly, Beck and coworkers reported that modification rates of three residues located in TM6 (residues 331, 333, and 335) near the predicted extracellular side by SH-modifying reagents exhibits state-dependent, where the rates of modification were 10-100-fold slower in the open state than in the closed state suggesting a conformational changes in TM6 is coupled to the gating mechanism that regulates the ion flow [132]. They also reported that modification of pore-lining residue 344 was not state-dependent, which is not consistent with our finding. In this study, they also used membrane permeant cation and SH-regent MTSEA, which could produce non-specific effects as reported by Smith et al. [79] and thereby

leading a misinterpretation of the results. Furthermore, maneuvers we used in this study to enhance P_O that lock open R334C-CFTR channels into the prominent **s2** subconductance state (Figures 15B and 17B). In contrast, Beck and coworkers attempted using cysteine substituted mutations coupled to E1371Q (NBD2) to enhance the P_O by prolonging the burst duration of these channels [132]. However, they did not examine the single-channel kinetics in a single cysteine substituted mutant channel. For example, R334C/E1371Q may exhibit a distinct different kinetics compared to R334C-CFTR activated by ATP + AMP-PNP or R334C/K1250A. It is completely possible that the difference between our observations and theirs is due to the different approaches regarding to the manipulation of P_O. Finally, our results also show that in R334C/K464A-CFTR, the rate of modification by $MTSET^+$ was increased dramatically presumably due to its low P_O (Fig. 18B); which is consistent with the notion that modification of R334C by $MTSET^+$ is strongly favored by closed state. Using the permeant anion $Au(CN)_2^-$ and SH-modifying reagents combined with cysteine substitution approaches, Fetehi and Linsdell reported that there are conformational changes in TM that occur in advance of channel opening, suggesting that multiple distinct closed pore conformation exist which is coupled with intracellular events at the R domain and/or NBDs [146].

In R334C-CFTR channels, the most stable conducting state is the **s2** state; while in WT-CFTR channels, the most stable conducting state is the f state (Figures 7, 8 and 9). Results from the present study show that when R334C-CFTR channels are locked open by either AMP-PNP or addition of the K1250A mutation, they are locked into the **s2** state. In contrast, previous studies show that WT-CFTR channels locked open by the same maneuvers are locked in the **f** state [34; 38; 157]. These observations suggest that the most stable conducting state of the pore reflects the fully-occupied, pre-hydrolytic state of the NBDs. Consistent with this notion, we recently reported that WT-CFTR channels locked open by either AMP-PNP or vanadate (and K1250A-CFTR channels with ATP alone) exhibit a reduced frequency of flickery closures compared to WT-CFTR channels in the presence of ATP alone [106]. R334C-CFTR channels almost always transition briefly to the f state before closure (Figures 7, 8, 9 and 17); the **f** state may represent an unstable conformation that serves as a transition intermediate

between the stable **s2** state and the stable **c** state. Hence, the stability of the open conductance states appears to be determined by the processes of binding and hydrolysis at the NBDs. The mechanism that couples conformational changes at the NBDs to conformational changes in the pore is an interesting subject for future study.

6. Summary and conclusions

CFTR functions as a small chloride channel, whose gating is controlled by binding and hydrolysis of ATP at nucleotide binding domains (NBDs). However, what forms the functional unit of CFTR and how binding and hydrolysis of ATP at NBDs drives the pore of CFTR to open and to close remain unclear. The studies proposed in this thesis attempted to address these questions utilizing the unique biophysical features of CFTRs bearing amino acid substitution in transmembrane domain (TM) six, combined with chemical modification. The magnitudes and distributions of subconductance states were studied in wild type CFTR and in mutated CFTRs in TM6. Within an open burst it was possible to distinguish three, distinct conductance states defined as the full conductance (**f**), subconductance 1 (**s1**) and subconductance 2 (**s2**). Amino acid substitutions in TM6 altered the duration and probability of occurrence of these subconductance states, but did not greatly alter their relative amplitudes. Covalent modification of single R334C-CFTR channels by $MTSET^+$, monitored in real-time, resulted in simultaneous modification of all three conductance levels in what appeared to be a single step, without altering the proportion of time spent in each state. This behavior suggested that at least a portion of the conduction path is common to all three conducting states. The time course for the modification of R334C-CFTR, measured in outside-out macropatches using a rapid perfusion system, was also consistent with a single modification step as if each pore contained only a single copy of the cysteine residue at position 334. These results suggest a model for the CFTR conduction pathway in which a single anion-conducting pore is formed by a single CFTR polypeptide.

We next used a similar approach combined with manipulation of the channel open probability to investigate changes in pore conformation that might accompany channel gating. In single R334C-CFTR channels studied in excised patches, modification by $MTSET^+$ occurred only during channel closed states. This suggests that the rate of reaction of the cysteine with $MTSET^+$ was greater in closed channels than in open channels. R334C-CFTR channels in outside-out macropatches activated by ATP alone were modified with first-order kinetics upon rapid exposure patch to $MTSET^+$.

Modification by $MTSET^+$ and $MTSES^-$ was much slower when channels were locked open by addition of non-hydrolyzable nucleotide AMP-PNP, or when the R334C mutation was coupled to a second mutation, K1250A, which greatly decreases channel closing rate. In contrast, modification was faster in R334C/K464A-CFTR channels, which exhibit prolonged interburst closed states. These data indicate that the reactivity of the engineered cysteine in R334C-CFTR is state-dependent, providing evidence of changes in pore conformation coupled to ATP binding and hydrolysis at the NBDs. The data also show that maneuvers that lock open R334C-CFTR do so by locking channels into the prominent **s2** subconductance state, suggesting that the most stable conducting state of the pore reflects the fully-occupied, pre-hydrolytic state of the NBDs. Taken together, our data demonstrated that the minimal functional unit is formed by a single CFTR polypeptide which composes a single pore and provided direct evidence that there is a conformational change in the outer vestibule of the pore associated with ATP-dependent gating events at the NBDs.

7. Acknowledgement

I would like to thank from the bottom of heart:

Dr. Nael A. McCarty, Associate Professor, Senior CF Scientist, Division of Pulmonology, Allergy/Immunology, Cystic Fibrosis, and Sleep Department of Pediatrics at Emory University School of Medicine, my mentor, who helped and supported my research work with great enthusiasm.

Dr. Darwin Bell, Professor and Head of the Renal Biology Laboratory at the Medical University of South Carolina, who supported my research work with great enthusiasm.

I would like to thank **Dr. László Rosivall**, Professor of Pathophysiology, Nephrology Research and Training Center, Institute of Pathophysiology, Faculty of Medicine, Semmelweis University, Budapest, Ph.D. program director, for helping me continuously along my career.

I am grateful to **Drs. H. Criss Hartzell and Douglas C. Eaton** at Emory University School of Medicine and **Dr. David C Dawson** at Oregon Health and Science University for a lot of helpful discussion about our research. I am also grateful to **Dr. Heping Ma,** Associate Professor at the University of Alabama at Birmingham for helping me in many aspects of my research career.

I would like to thank my colleagues at the Medical University of South Carolina and Emory University for their help and the friendly atmosphere.

Finally, I dedicate my work to Binlin Song, my wife who prepared all mutations for this study; I dedicate my work to Mom, my children, Yuandi and Crystal.

8. Bibliography

1. Riordan JR, Rommens JM,.Kerem B-S, Alon N, Rozmahel R, Grzelczak Z, Zielenski J, Lok S, Plavsic N, Chou J-L, Drumm ML, Iannuzzi MC, Collins FS, Tsui L-C (1989) Identification of the cystic fibrosis gene: cloning and characterization of complementary DNA. *Science,* **245**:1066-1072.

2. Higgins CF. (1995) The ABC of channel regulation. *Cell,* 82:693-696.

3. Guggino WB, Stanton BA. (2006) New insights into cystic fibrosis: molecular switches that regulate CFTR. *Nat Rev Mol Cell Biol*., **7**(6):426-36.

4. Welsh MJ, Ramsey BW (1998) Research on cystic fibrosis: a journey from the Heart House. *Am J Respir Crit Care Med.,* **157**(4 Pt 2):S148-54.

5. Higgins CF. (1995) P-glycoprotein and cell volume-activated chloride channels. *J Bioenerg Biomembr.,* **27**(1):63-70.

6. Schwiebert EM,. Benos DJ, Egan ME, Stutts MJ, Guggino WB. (1999) CFTR is a conductance regulator as well as a chloride channel. Physiol Rev., 1999 Jan;**79**(1 Suppl):S145-66.

7. McCarty NA, Zhang Z-R (2001) Identification of a region of strong discrimination in the pore of CFTR. *Am. J. Physiol.*, Lung **281**:L852-L867.

8. Stutts MJ, Lazarowski ER, Paradiso AM, Boucher RC. (1995) Activation of CFTR Cl- conductance in polarized T84 cells by luminal extracellular ATP. *Am J Physiol Cell Physiol.,* **268**: C425-C433

9. McNicholas CM, Nason MW Jr, Guggino WB, Schwiebert EM, Hebert SC, Giebisch G, Egan ME. (1997) A functional CFTR-NBF1 is required for ROMK2-CFTR interaction. *Am J Physiol Renal Physiol.*, **273**: F843-F848**.**

10. Ishida-Takahashi A, Otani H, Takahashi C, Washizuka T, Tsuji K, Noda M, Horie M, Sasayama S. (1998) Cystic fibrosis transmembrane conductance regulator mediates sulphonylurea block of the inwardly rectifying K+ channel Kir6.1. *J Physiol.,* **508**:23-30

11. Schwiebert EM, Egan ME, Guggino WB. (1998) Assays of dynamics, mechanisms, and regulation of ATP transport and release: implications for study of ABC transporter function. *Methods Enzymol.,* **292**:664-75.

12. Jouret F, Bernard A, Hermans C, Dom G, Terryn S, Leal T, Lebecque P, Cassiman JJ, Scholte BJ, de Jonge HR, Courtoy PJ, Devuyst O. (2007) Cystic fibrosis is associated with a defect in apical receptor-mediated endocytosis in mouse and human kidney. *J Am Soc Nephrol.,* **18**(3):707-18.

13. Hume JR, Duan D, Collier ML, Yamazaki J, Horowitz B. (2000). Anion transport in heart. *Physiological Reviews,* **80**: 31-81.

14. Moss AJ. (1982). The cardiovascular system in cystic fibrosis. *Pediatrics,* **70**: 728-41.

15. Zebrak J, Skuza B, Pogorzelski A, Ligarska R, Kopytko E, Pawlik J, Rutkiewicz E, Witt M. (2000). Partial CFTR genotyping and characterization of cystic fibrosis patients with myocardial fibrosis and necrosis. *Clin Genet*, **57:** 56-60.

16. Mendoza JL, Thomas PJ. (2007) Building an understanding of cystic fibrosis on the foundation of ABC transporter structures. *J Bioenerg Biomembr,* **39**:499-505.

17. Anderson MP, Berger HA, Rich DP, Gregory RJ, Smith AE, Welsh MJ. (1991) Nucleoside triphosphates are required to open the CFTR chloride channel. *Cell,* **67**(4):775-84.

18. Nagel G, Hwang TC, Nastiuk KL, Nairn AC, Gadsby DC. (1992) The protein kinase A-regulated cardiac Cl- channel resembles the cystic fibrosis transmembrane conductance regulator. *Nature,* **360**(6399):81-4.

19. Rich DP, Gregory RJ, Anderson MP, Manavalan P, Smith AE, Welsh MJ. (1991) Effect of deleting the R domain on CFTR-generated chloride channels. *Science,* **253**(5016):205-7.

20. Csanády L, Chan KW, Seto-Young D, Kopsco DC, Nairn AC, Gadsby DC. (2000) Severed channels probe regulation of gating of cystic fibrosis transmembrane conductance regulator by its cytoplasmic domains. *J Gen Physiol.,* **116**(3):477-500.

21. Bompadre SG, Cho JH, Wang X, Zou X, Sohma Y, Li M, Hwang TC. (2005) CFTR gating II: Effects of nucleotide binding on the stability of open states. *J Gen Physiol.,* **125**(4):377-94.

22. Ikuma M, Welsh MJ. (2000) Regulation of CFTR Cl^- channel gating by ATP binding and hydrolysis. *Proc.Natl.Acad.Sci.,USA,* **97**:8675-8680.

23. Zeltwanger S, Wang F, Wang G-T, Gillis KD, Hwang T-C. (1999) Gating of cystic fibrosis transmembrane conductance regulator chloride channels by adenosine triphosphate hydrolysis: Quantitative analysis of a cyclic gating scheme. *J.Gen.Physiol.,* **113**:541-554.

24. Zou X, Hwang T-C. (2001) ATP hydrolysis-coupled gating of CFTR chloride channels: structure and function. *Biochemistry*, **40**:5579-5586.

25. Vergani P, Lockless SW, Nairn AC, Gadsby DC. (2005) CFTR channel opening by ATP-driven tight dimerization of its nucleotide-binding domains.
Nature, **433**, 876-880.

26. Gadsby DC, Vergani P, Csanády L. (2006) The ABC protein turned chloride channel whose failure causes cystic fibrosis. *Nature,* **440**(7083):477-83.

27. Chang G. (2003) Structure of MsbA from *Vibrio cholera*: a multidrug resistance ABC transporter homolog in a closed conformation. *J.Mol.Biol,* **330**:419-430.

28. Chang G, Roth CB. (2001) Structure of MsbA from *E. coli*: a homolog of the multidrug resistance ATP binding cassette (ABC) transporters. *Science,* **293**:1793-1800

29. Chen J, Lu G, Lin J, Davidson AL, Quiocho FA. (2003) A tweezers-like motion of the ATP-binding cassette dimer in an ABC transport cycle. *Mol.Cell,* **12**:651-661.

30. Lewis HA, Buchanan SG, Burley SK, Conners K, Dickey M, Dorwart M, Fowler R, Gao X, Guggino WB, Hendrickson WA, Hunt JF, Kearins MC, Lorimer D, Maloney PC, Post KW, Rajashankar KR, Rutter ME, Sauder JM, Shriver S, Thibodeau PH, Thomas PJ, Zhang M, Zhao X, Emtage S. (2004) Structure of nucleotide-binding domain 1 of the cystic fibrosis transmembrane conductance regulator. *EMBO J.*, **23**:282-93.

31. Locher KP, Lee AT, Rees DC. (2002) The *E. coli* BtuCD structure: a framework for ABC transporter architecture and mechanism. *Science,* **296**:1091-1098.

32. Kidd JF, Ramjeesingh M, Stratford F, Huan LJ, Bear CE. (2004) A heteromeric complex of the two nucleotide binding domains of CFTR mediates ATPase activity. *J.Biol.Chem.,* **279**(40):41664-9.

33. Basso C, Vergani P, Nairn AC, Gadsby DC. (2003) Prolonged nonhydrolytic interaction of nucleotide with CFTR's NH_2-terminal nucleotide binding domain and its role in channel gating. *J.Gen.Physiol.,* **122**:333-348.

34. Vergani P, Nairn AC, Gadsby DC. (2003) On the mechanism of MgATP-dependent gating of CFTR Cl^- channels. *J.Gen.Physiol.*, **120**:17-36.

35. Ramjeesingh M, Li C, Garami E, Huan LJ, Galley K, Wang Y, Bear CE. (1999) Walker mutations reveal loose relationship between catalytic and channel-gating activities of purified CFTR (cystic fibrosis transmembrane conductance regulator). *Biochemistry.,* **38**(5):1463-8.

36. Powe AC Jr, Al-Nakkash L, Li M, Hwang TC. (2002) Mutation of Walker-A lysine 464 in cystic fibrosis transmembrane conductance regulator reveals functional interaction between its nucleotide-binding domains. *J Physiol.,* **539**(Pt 2):333-46.

37. Zhou Z, Wang X, Liu HY, Zou X, Li M, Hwang TC. (2006) The two ATP binding sites of cystic fibrosis transmembrane conductance regulator (CFTR) play distinct roles in gating kinetics and energetics. *J Gen Physiol.,* **128**(4):413-22.

38. Carson MR, Travis SM, Welsh MJ. (1995) The two nucleotide-binding domains of cystic fibrosis transmembrane conductance regulator (CFTR) have distinct functions in controlling channel activity. *J Biol Chem.,* **270**(4):1711-7.

39. Gunderson KL, Kopito RR. (1995) Conformational states of CFTR associated with channel gating: the role ATP binding and hydrolysis. *Cell,* **82**(2):231-9.

40. Berger AL, Ikuma M, Welsh MJ. (2005) Normal gating of CFTR requires ATP binding to both nucleotide-binding domains and hydrolysis at the second nucleotide-binding domain. *Proc Natl Acad Sci. U S A.,* **102**(2):455-60.

41. Bompadre SG, Hwang TC. (2007) Cystic fibrosis transmembrane conductance regulator: a chloride channel gated by ATP binding and hydrolysis. *Sheng Li Xue Bao.,* **59**(4):431-42.

42. Wang W, Bernard K, Li G, Kirk KL. (2007) Curcumin opens cystic fibrosis transmembrane conductance regulator channels by a novel mechanism that requires neither ATP binding nor dimerization of the nucleotide-binding domains.
J Biol Chem., **282**(7):4533-44.

43. Dawson DC, Smith SS, Mansoura MK, (1999). CFTR: Mechanism of anion conduction. *Physiol. Rev*., **79**, S47-S45

44. Anderson MP, Gregory RJ, Thompson S, Souza DW, Paul S, Mulligan RC, Smith AE, Welsh MJ. (1991) Demonstration that CFTR is a chloride channel by alteration of its anion selectivity. *Science,* **253**:202-5.

45. Gong X, Linsdell P. (2004) Maximization of the rate of chloride conduction in the CFTR channel pore by ion-ion interactions. *Arch Biochem Biophys.,* **426**(1):78-82.

46. Liu X, Smith SS, Dawson DC. (2003) CFTR: what's it like inside the pore? *J Exp Zoolog A Comp Exp Biol.,* **300**(1):69-75.

47. Linsdell P, Tabcharani JA, Rommens JM, Hou YX, Chang XB, Tsui LC, Riordan JR, Hanrahan JW. (1997) Permeability of wild-type and mutant cystic fibrosis transmembrane conductance regulator chloride channels to polyatomic anions. . *J.Gen.Physiol.,* **110**:355-64.

48. Gong X, Burbridge SM, Cowley EA, Linsdell P. (2002) Molecular determinants of Au(CN)(2)(-) binding and permeability within the cystic fibrosis transmembrane conductance regulator Cl(-) channel pore. *J Physiol.,* **540**(Pt 1):39-47.

49. Linsdell P, Hanrahan JW. (1996) Flickery block of single CFTR chloride channel by intracellular anions and osmolytes. *Am. J. Physiol*., **271**:C628-34.

50. Linsdell P, Hanrahan JW. (1998) Adenosine triphosphate-dependent asymmetry of anion permeation in the cystic fibrosis transmembrane conductance regulator chloride channel. *J.Gen.Physiol.,* **111**:601-614.

51. Linsdell P, Hanrahan JW. (1998) Glutathione permeability of CFTR. *Am. J. Physiol*., **275**:C323-26.

52. Khakh BS, Lester HA. (1999) Dynamic selectivity filters in ion channels. *Neuron* ,**23**:653-58.

53. Sheppard DN, Welsh MJ. (1999) Structure and function of the CFTR chloride channel. *Physiol Rev.,* **79**(1 Suppl):S23-45.

54. Price MP, Ishihara H, Sheppard DN, Welsh MJ. (1996) Function of Xenopus cystic fibrosis transmembrane conductance regulator (CFTR) Cl channels and use of human-Xenopus chimeras to investigate the pore properties of CFTR. *J Biol Chem.,* **271**(41):25184-91.

55. Sheppard DN, Ostedgaard LS, Rich DP, Welsh MJ. (1994) The amino-terminal portion of CFTR forms a regulated Cl- channel. *Cell,* **76**(6):1091-8.

56. Carroll TP, Morales MM, Fulmer SB, Allen SS, Flotte TR, Cutting GR, Guggino WB. (1995) Alternate translation initiation codons can create functional forms of cystic fibrosis transmembrane conductance regulator. *J Biol Chem.,* **270**(20):11941-6.

57. Morales MM, Carroll TP, Morita T, Schwiebert EM, Devuyst O, Wilson PD, Lopes AG, Stanton BA, Dietz HC, Cutting GR, Guggino WB. (1996) Both the wild type and a functional isoform of CFTR are expressed in kidney. *Am J Physiol.,* **270**(6 Pt 2):F1038-48.

58. Devidas S, Yue H, Guggino WB. (1998) The second half of the cystic fibrosis transmembrane conductance regulator forms a functional chloride channel. *J Biol Chem.,* **273**(45):29373-80

59. Marshall J, Fang S, Ostedgaard LS, O'Riordan CR, Ferrara D, Amara JF, Hoppe H 4th, Scheule RK, Welsh MJ, Smith AE. (1994) Stoichiometry of recombinant cystic fibrosis transmembrane conductance regulator in epithelial cells and its functional reconstitution into cells in vitro. *J Biol Chem.,* **269**(4):2987-95.

60. Tao T, Xie J, Drumm ML, Zhao J, Davis PB, Ma JJ. Slow conversions among subconductance states of cystic fibrosis transmembrane conductance regulator chloride channel. (1996) *Biophys J*., **70**:743-53.

61. Zerhusen B, Zhao JY, Xie JX, Davis PB, Ma JJ. (1999) A single conductance pore for chloride ions formed by two cystic fibrosis transmembrane conductance regulator molecules. *J. Biol Chem*., **274**:7627-7630.

62. Eskandari S, Wright EM, Kreman M, Starace DM, Zampighi GA. (1998) Structural analysis of cloned plasma membrane proteins by freeze-fracture electron microscopy. *Proc Natl Acad Sci U S A.,* **95**(19):11235-40

63. Nikaido K, Liu PQ, Ames GF. (1997) Purification and characterization of HisP, the ATP-binding subunit of a traffic ATPase (ABC transporter), the histidine permease of

Salmonella typhimurium. Solubility, dimerization, and ATPase activity. *J Biol Chem.,* **272**(44):27745-52.

64. Hung LW, Wang IX, Nikaido K, Liu PQ, Ames GF, Kim SH. (1998) Crystal structure of the ATP-binding subunit of an ABC transporter. *Nature,* **396**(6712):703-7.

65. Devidas S, Guggino WB. (1998) CFTR: domains, structure, and function. *J Bioenerg Biomembr.,* **29**(5):443-51.

66. Gallet X, Festy F, Ducarme P, Brasseur R, Thomas-Soumarmon A. (1998) Topological model of membrane domain of the cystic fibrosis transmembrane conductance regulator. *J Mol Graph Model.*, **16**(2):72-82, 97-8.

67. Montal M, Montal MS, Tomich JM. (1990) Synporins--synthetic proteins that emulate the pore structure of biological ionic channels. *Proc Natl Acad Sci U S A.,* **87**(18):6929-33.

68. Oblatt-Montal M, Reddy GL, Iwamoto T, Tomich JM, Montal M.(1994) Identification of an ion channel-forming motif in the primary structure of CFTR, the cystic fibrosis chloride channel. *Proc Natl Acad Sci U S A.*, **91**(4):1495-9.

69. Cheung M, Akabas MH (1996) Identification of cystic fibrosis transmembrane conductance regulator channel-lining residues in and flanking the M6 membrane-spanning segment. *Biophys J.,* **70**(6):2688-95.

70. Cheung M, Akabas MH. (1997) Locating the anion-selectivity filter of the cystic fibrosis transmembrane conductance regulator (CFTR) chloride channel. *J Gen Physiol.,* **109**(3):289-99.

71. Rosenberg MF, Kamis AB, Aleksandrow LA, Ford RC, Riordan JR. (2005). Purification and crystallization of the cystic fibrosis transmembrane conductance regulator (CFTR). *J.Biol.Chem.,* **279**:39051-7.

72. Linsdell P, Zheng SX, Hanrahan JW. (1998) Non-pore lining amino acid side chains influence anion selectivity of the human CFTR Cl- channel expressed in mammalian cell lines. *J. Physiol*., **512**:1-16.

73. Tabcharani JA, Linsdell P, Hanrahan JW. (1997) Halide permeation in wild-type and mutant cystic fibrosis transmembrane conductance regulator chloride channels. *J.Gen.Physiol.,* **110**:431-54.

74. Linsdell P, Evagelidis A, Hanrahan JW. (2000) Molecular determinants of anion selectivity in the cystic fibrosis transmembrane conductance regulator chloride channel pore. *Biophys J*., **78**:2973-82.

75. Mansoura MK, Smith SS, Choi AD, Richards NW, Strong TV, Drumm ML, Collins FS, Dawson DC. (1998) Cystic fibrosis transmembrane conductance regulator (CFTR) anion binding as a probe of the pore. *Biophys J*., **74(3)**:1320-1332.

76. McDonough S, Davidson N, Lester HA, McCarty NA. (1994) Novel pore-lining residues in CFTR that govern permeation and open-channel block. *Neuron,* **13**:623-634.

77. Tabcharani JA, Rommens JM, Hou YX, Chang XB, Tsui LC, Riordan JR, Hanrahan JW. (1993) Multi-ion pore behaviour in the CFTR chloride channel. *Nature,* **366**(6450):79-82.

78. Cotten JF, Welsh MJ. (1999) Cystic fibrosis-associated mutations at arginine 347 alter the pore architecture of CFTR. Evidence for disruption of a salt bridge. *J.Biol.Chem.,* **247**(9):5429-5435.

79. Smith SS, Liu X,. Zhang Z-R, Sun F, Kriewall TE, McCarty NA, Dawson DC. (2001) CFTR: Covalent and noncovalent modification suggests a role for fixed charges in anion conduction. *J.Gen.Physiol.,* **118**:407-431.

80. Lester HA. (1991) Strategies for studying permeation at voltage-gated ion channels. *Annu. Rev. Physiol.,* **53**:477-496.

81. Lester HA. (1988) Heterologous expression of excitability proteins: route to more specific drugs? *Science,* **241**:1057-1063.

82. Leonard RJ, Labarca CG, Charnet P, Davidson N, Lester HA. (1988) Evidence that the M2 membrane-spanning region lines the ion channel pore of the nicotinic receptor. *Science,* **242**:1578-1581.

83. McCarty NA. (2000) Permeation through the CFTR chloride channel. *J.Exp.Biol.,* **203**:1947-1962.

84. Zhang Z-R, Zeltwanger S, McCarty NA. (2000) Direct comparison of NPPB and DPC as probes of CFTR expressed in *Xenopus* oocytes. *J.Membr.Biol,* **175**:35-52.

85. Walsh KB, Wang C. (1998) Arylaminobenzoate block of the cardiac cyclic AMP-dependent chloride current. *Mol Pharmacol,* **53(3)**:539-46.

86. McCarty NA, McDonough S, Cohen BN, Riordan JR, Davidson N, Lester HA. (1993) Voltage-dependent block of the cystic fibrosis transmembrane conductance regulator Cl^- channel by two closely related arylaminobenzoates. *J.Gen.Physiol.,* **102**:1-23.

87. Zhang Z-R, McDonough SI, McCarty NA. (2000) Interaction between permeation and gating in a putative pore-domain mutant in CFTR. *Biophys.J.,* **79**:298-313.

88. Mehnert H, Karg E. (1969) Glibenclamide (HB 419): a new oral antidiabetic of sulphonylurea type. *Ger Med Mon.,* **14**(8):373-7.

89. Schultz BD, DeRoos AD, Venglarik CJ, Singh AK, Frizzell RA, Bridges RJ. (1996) Glibenclamide blockade of CFTR chloride channels. *Am J Physiol*., **271**(2 Pt 1):L192-200.

90. Sheppard DN, Robinson KA. (1997) Mechanism of glibenclamide inhibition of cystic fibrosis transmembrane conductance regulator Cl- channels expressed in a murine cell line. *J Physiol*., **503**(Pt 2):333-46.

91. Zhang Z-R, Zeltwanger S, McCarty NA. (2004) Steady-state interaction of glibenclamide with CFTR: evidence for multiple sites. *J.Membr.Biol*, **199**:15-28.

92. Zhang Z-R, Cui G., Zeltwanger S, McCarty NA. (2004) Time-dependent interactions of glibenclamide with CFTR: Kinetically complex block of macroscopic currents. *J.Membr.Biol*., **201(3)**:139-55.

93. Zhou Z, Hu S, Hwang T-C. (2002). Probing an open CFTR pore with organic anion blockers. *J. Gen. Physiol.,* **120**:647-662.

94. Linsdell P, Hanrahan JW. (1996) Disulphonic stilbene block of cystic fibrosis transmembrane conductance regulator Cl- channels expressed in a mammalian cell line and its regulation by a critical pore residue. *J. Physiol (Lond),* **496**:687-693.

95. Armstrong CM, Binstock L. (1965) Anomalous rectification in the squid giant axon injected with tetraethylammonium chloride. *J.Gen.Physiol.,* **48**:859-872.

96. Armstrong CM. (1966) Time course of TEA(+)-induced anomalous rectification in squid giant axons. *J.Gen.Physiol.,* **50**:491-503.

97. Armstrong CM. (1969) Inactivation of the potassium conductance and related phenomena caused by quaternary ammonium ion injection in squid axons. *J.Gen.Physiol.,* **54**:553-575.

98. Armstrong CM. (1971) Interaction of tetraethylammonium ion derivatives with the potassium channels of giant axons. *J.Gen.Physiol.,* **58**:413-437.

99. Ward A, Reyes CL, Yu J, Roth CB, Chang G. (2007) Flexibility in the ABC transporter MsbA: Alternating access with a twist. *Proc Natl Acad Sci U S A.*, **104**(48):19005-10.

100. Muanprasat C, Sonawane ND, Salinas D, Taddei A, Galietta LJ, Verkman AS. (2004) Discovery of glycine hydrazide pore-occluding CFTR inhibitors: mechanism, structure-activity analysis, and in vivo efficacy. *J.Gen.Physiol.,* **124**:125-37.

101. Castle NA, Haylett DG, Jenkinson DH. (1989) Toxins in the characterization of potassium channels. *Trends Neurosci.,* **12**(2):59-65.

102. Possani LD, Merino E, Corona M, Bolivar F, Becerril B. (2000) Peptides and genes coding for scorpion toxins that affect ion-channels. *Biochimie*., **82**(9-10):861-8.

103. French RJ, Dudley SC Jr. (1999) Pore-blocking toxins as probes of voltage-dependent channels. *Methods Enzymol.,* **294**:575-605.

104. Lewis RJ, Garcia ML. (2003) Therapeutic potential of venom peptides. *Nat Rev Drug Discov.*, **2(**10):790-802.

105. Fuller MD, Zhang Z-R, Cui G, McCarty NA. (2004). CFTR Channel Inhibition by a Peptide Toxin of Scorpion Venom. *Am. J. Physiol* (*Cell Physiol)*, **287**(5): C1328-C1341.

106. Fuller MD, Zhang Z-R, Cui G, McCarty NA. (2005) The block of CFTR by scorpion is state dependent. *Biophys. J.,* **89**(6):3960-75

107. Fuller MD, Thompson CH, Zhang Z-R, McMaster D, French RJ, Pohl J, Kubanek J, McCarty NA. (2007) Inhibition of CFTR chloride channels by a novel peptide toxin. *J. Biol. Chem.,* **282**(52):37545-55

108. Serohijos AW, Hegedus T, Aleksandrov AA, He L, Cui L, Dokholyan NV, Riordan JR. (2008) Phenylalanine-508 mediates a cytoplasmic-membrane domain contact in the CFTR 3D structure crucial to assembly and channel function. *Proc Natl Acad Sci U S A.,* **105**(9):3256-61

109. Younger JM, Chen L, Ren HY, Rosser MF, Turnbull EL, Fan CY, Patterson C, Cyr DM. (2006) Sequential quality-control checkpoints triage misfolded cystic fibrosis transmembrane conductance regulator. *Cell,* **126**(3):571-82.

110. Cui L, Aleksandrov L, Chang XB, Hou YX, He L, Hegedus T, Gentzsch M, Aleksandrov A, Balch WE, Riordan JR. (2007) Domain interdependence in the biosynthetic assembly of CFTR. *J Mol Biol.,* **365**(4):981-94.

111. Serrano L, Bycroft M, Fersht AR. (1991) Aromatic-aromatic interactions and protein stability. Investigation by double-mutant cycles. *J Mol Biol.,* **218**(2):465-75.

112. McGaughey GB, Gagné M, Rappé AK. (1998) pi-Stacking interactions. Alive and well in proteins. *J Biol Chem*., **273**(25):15458-63.

113. Stauffer DA, Karlin A. (1994) Electrostatic potential of the acetylcholine binding sites in the nicotinic receptor probed by reactions of binding-site cysteines with charged methanethiosulfonates. *Biochemistry.,* **33**(22):6840-9.

114. Liu, Y. M. E. Jurman, and G. Yellen. Dynamic rearrangement of the outer mouth of a K+ channel during gating. (1996). *Neuron*, **16**:859-867

115. Pascual JM, Karlin A. (1998). State-dependent accessibility and electrostatic potential in the channel of the acetylcholine receptor. Inferences from rates of reaction of thiosulfonates with substituted cysteines in the M2 segment of the alpha subunit. *J. Gen. Physiol*, **111**:717-739.

116. Snyder PM, Bucher DB, Olson DR. (2000) Gating induces a conformational change in the outer vestibule of ENaC. *J. Gen. Physio*l., **116**:781-790.

117. Flynn GE, Johnson JP, Zagotta WN. (2001) Cyclic nucleotide-gated channels: shedding light on the opening of a channel pore. *Nature Reviews*, **2**(9):643-652.

118. Cui Y, Fan Z. (2002) Mechanism of Kir6.2 channel inhibition by sulfhydryl modification: pore block or allosteric gating? *J. of Physiol*. **540**(3):731-741.

119. Flynn GE, Zagotta WN. (2003). A cysteine scan of the inner vestibule of cyclic nucleotide-gated channels reveals architecture and rearrangement of the pore. *J. Gen. Physiol*., 121:563-582.

120. Trapp S, Haider S, Jones P, Sansom SP, Ashcroft FM. (2003) Identification of residues contributing to the ATP binding site of Kir6.2. *The EMBO J*., **22**(12):2903-12.

121. Chen M-F, Chen T-Y. (2003) Side-chain charge effects and conductance determinants in the pore of ClC-0 chloride channels. *J. Gen. Physiol*., **122**:133-145.

122. Lin C-W, Chen T-Y. (2003) Probing the pore of ClC-0 by substituted cysteine accessibility method using methane thiosulfonate reagents. *J. Gen. Physiol*., **122**:147-159.

123. Latorre R, Olcese R, Basso C, Gonzalez C, Munoz F, Cosmelli D, Alvarez O. (2003) Molecular coupling between voltage sensor and pore opening in the Arabidopsis inward rectifier K+ channel KAT1. *J. Gen. Physiol*., **122**:459-469.

124. Akabas MH, Kaufmann C, Cook TA, Archdeacon P. (1994). Amino acid residues lining the chloride channel of the cystic fibrosis transmembrane conductance regulator. *J Biol Chem*., **269**(21): 14865-8.

125. Akabas MH. (1998). Channel-lining residues in the M3 membrane-spanning segment of the cystic fibrosis transmembrane conductance regulator. *Biochemistry*, **37**(35): 12233-12240.

126. Akabas MH, Cheung M, Guinamard R. (1997). Probing the structural and functional domains of the CFTR chloride channel. *J. Bioenerg Biomember*., **25**(5):453-63.

127. Guinamard R, Akabas MH. (1999). Arg352 is a major determinant of charge selectivity in the cystic fibrosis transmembrane conductance regulator chloride channel. *Biochemistry*. **38**(17): 5528-37.

128. Liu X, Serrano J, Fuller MD, Zhang Z-R, Alexander C, McCarty NA, Dawson DC. (2004). CFTR: Sizing the vestibule of the pore by covalent modification of engineered cysteines. *Biophys. J.,* **86**:284a

129. Zhang Z-R, Song B, McCarty NA. (2005) State-dependent modification of R334C by $MTSET^+$ reveals conformational change in the outer vestibule of CFTR. *J. Biol. Chem.,* **280**(51):41997-42003.

130. Zhang Z-R, Cui G, Liu X, Song B., Dawson DC, McCarty NA. (2005) Determination of the functional unit of the CFTR chloride channel: One polypeptide forms one pore. *J. Biol. Chem.,* **280**(1):458-468.

131. McCarty NA, Zhang Z-R. (2001) Identification of a region of strong discrimination in the pore of CFTR. *Am. J. Physiol. Lung*, **281**: L852-L867.

132. Beck EJ, Yang Y, Yaemsiri S, Raghuram V. (2007) Conformational changes in a pore-lining helix coupled to cystic fibrosis transmembrane conductance regulator channel gating. *J Biol Chem.,* **283**(8):4957-66.

133. Middleton RE, Pheasant DJ, Miller C. (1994) Purification, reconstitution, and subunit composition of a voltage-gated chloride channel from Torpedo electroplax. *Biochemistry,* **33**(45):13189-98.

134. Middleton RE, Pheasant DJ, Miller C. (1996) Homodimeric architecture of a ClC-type chloride ion channel. *Nature,* **383**(6598):337-40.

135. Ludewig U, Jentsch TJ, Pusch M. (1997) Inward rectification in ClC-0 chloride channels caused by mutations in several protein regions. *J Gen Physiol.,* **110**(2):165-71.

136. Yue H, Devidas S, Guggino WB. (2000) The two halves of CFTR form a dual-pore ion channel. *J Biol Chem.,* **275**(14):10030-4.

137. Harrington MA, Kopito RR. (2002) Cysteine residues in the nucleotide binding domains regulate the conductance state of CFTR channels. *Biophys.J.,* **82**:1278-1292.

138. Ishihara H, Welsh MJ. (1997) Block by MOPS reveals a conformation change in the CFTR pore produced by ATP hydrolysis. *Am J Physiol.,* **273**(4 Pt 1):C1278-89.

139. Kogan I, Ramjeesingh M, Huan LJ, Wang Y, Bear CE. (2001) Perturbation of the pore of the cystic fibrosis transmembrane conductance regulator (CFTR) inhibits its atpase activity. *J Biol Chem.,* **276**(15):11575-81.

140. Bernèche S, Roux B. (2001) Energetics of ion conduction through the K^+ channel. *Nature,* **414**:73-77.

141. Seibert FS, Linsdell P, Loo TP, Hanrahan JW, Clarke DM, Riordan JR. (1996) Disease-associated mutations in the fourth cytoplasmic loop of cystic fibrosis transmembrane conductance regulator compromise biosynthetic processing and chloride channel activity. *J. Biol. Chem.,* **271**:15139-15145.

142. Seibert FS, Linsdell P, Loo TW, Hanrahan JW, Riordan JR, Clarke DM. (1996) Cytoplasmic loop three of cystic fibrosis transmembrane conductance regulator contributes to regulation of chloride channel activity. *J.Biol.Chem.,* **271**:27493-27499.

143. Xie J, Drumm ML, Ma J, Davis PB. (1995) Intracellular loop between transmembrane segments IV and V of cystic fibrosis transmembrane conductance regulator is involved in regulation of chloride channel conductance state. *J.Biol.Chem.*, **270**:28084-28091.

144. Zhang Z-R, McDonough S, McCarty NA. (2000) Interaction between Permeation and Gating in a Putative Pore- domain Mutant in CFTR. *Biophys. J.,* **79**, 298-313.

145. Zhang Z-R, Zeltwanger S, Smith SS, Dawson DC, McCarty NA. (2000) CFTR: A mutation in TM5 (V317E) results in voltage-dependent open probability. *Biophys.J.,* **78**:467A

146. Fatehi M, Linsdell P. (2007) State-dependent Access of Anions to the Cystic Fibrosis Transmembrane Conductance Regulator Chloride Channel Pore. *J Biol Chem.,* **283**(10):6102-9.

147. Zhang Z-R, McCarty NA. (2002) Determination of the oligomeric structure of functional CFTR chloride channels. *Biophys. J.,* **82**:240a

148. Haws C, Krouse ME, Xia Y, Gruenert DC, Wine JJ. (1992) CFTR channels in immortalized human airway cells. *Am. J. Physiol*., **263**: L692-L707

149. Linsdell P, Zheng SX, Hanrahan JW. (1998) Non-pore lining amino acid side chains influence anion selectivity of the human CFTR chloride channel expressed in mammalian cell lines. *J. Physiol. (Lond)*., **512**:1-16.

150. Fox JA. (1987) Ion channel subconductance states. *J. Membr. Biol*., **97**(1):1-8.

151. Laver DR, Peter WG. (1997) Interpretation of substates in ion channels: Unipores or multipores? *Prog. Biophys. Molec. Biol*., **67**:99-140.

152. Liu X, Smith SS, Sun F, Dawson DC. (2001) CFTR: Covalent modification of cysteine-substituted channels expressed in *Xenopus oocytes* shows that activation is due to the opening of channels resident in the plasma membrane. *J. Gen. Physiol*., **118**: 433-446.

153. Lin C-W, Chen T-Y. (2000) Cysteine modification of a putative pore residue in ClC-0: Implication for the pore stoichiometry of ClC chloride channels. *J. Gen. Physiol.,* **116**:535-546.

154. Liu X, Zhang Z-R, Fuller MD, Billingsly J, McCarty NA, Dawson DC. (2004) CFTR: A cysteine at 338 senses a positive electrostatic potential in the pore. *Biophys. J*., **87**(6):3826-3841.

155. Yang AS, Gunner MR, Sampogna R, Sharp K, Honig B. (1993) On the calculation of pK_as in proteins. *Proteins*, **15**(3): 252-65.

156. Antosiewicz J, McCammon JA, Gilson MK. (1994) Prediction of pH-dependent properties of proteins. *J. Mol. Biol*., **238**(3): 415-36.

157. Powe AC Jr, Al-Nakkash L, Li M, Hwang T-C. (2002) Mutation of Walker-A lysine 464 in cystic fibrosis transmembrane conductance regulator reveals functional interaction between its nucleotide-binding domains. *J. Physiol*., **539**, 333-46.

158. Hwang T-C, Nagel G, Nairn AC, Gadsby DC. (1994) Regulation of the gating of cystic fibrosis transmembrane conductance regulator C1 channels by phosphorylation and ATP hydrolysis. *Proc. Natl. Acad. Sci. U.S.A*., **91**:4698–4702.

159. Gadsby DC, Dousmanis AG, Nairn AC. (1998) Regulation of the gating of cystic fibrosis transmembrane conductance regulator C1 channels by phosphorylation and ATP hydrolysis. *Acta Physiol. Scand. Suppl*., **643**, 247-56.

160. Chen JH, Chang XB, Aleksandrov AA, Riordan JR. (2002) CFTR is a monomer: Biochemical and functional evidence. *J. Membr Biol.,* **188**: 55-71.

161. Wang S, Yue H, Derin RB, Guggino WB, Li M. (2000) Accessory protein facilitated CFTR-CFTR interaction, a molecular mechanism to potentiate the chloride channel activity. *Cell*, **103**:169-79

162. Raghuram V, Mak DO, Foskett JK. (2001) Regulation of cystic fibrosis transmembrane conductance regulator single-channel gating by bivalent PDZ-domain-mediated interaction. *Proc Natl Acad Sci U S A*., **98**: 1300-1305.

163. Ramjeesingh M, Ugwu F, Li C, Dhani S, Huan LJ, Wang Y, Bear CE. (2003) Stable dimeric assembly of the second membrane-spanning domain of CFTR (cystic fibrosis transmembrane conductance regulator) reconstitutes a chloride-selective pore. *Biochemistry,* **375**: 633-641.

164. Chan KW, Csanady L, Seto-Young D, Nairn AC, Gadsby DC. (2000) Severed molecules functionally define the boundaries of the cystic fibrosis transmembrane conductance regulator's NH_2-terminal nucleotide binding domain. *J Gen Physiol*., **116**: 163-80.

165. Schillers H, Shahin V, Albermann L, Schafer C, Oberleithner H (2004) Imaging CFTR: A tail to tail dimer with a central pore. *Cell Physiol. Biochem.,* **14**:1-10.

166. Doyle DA, Cabral JM, Pfuetzner RA, Kuo A, Gulbis JM, Cohen SL, Chait BT, MacKinnon R. (1998) The structure of the potassium channel: Molecular basis of K^+ conduction and selectivity. *Science,* **280**:69-77.

167. Gong X, Linsdell P. (2003) Molecular determinants and role of an anion binding site in the external mouth of the CFTR chloride channel pore. *J. Physiol.,* **549**: 387-397.

168. Ramjeesingh M, Li C, Kogan I, Wang Y, Huan LJ, Bear CE. (2001) A monomer is the minimum functional unit required for channel and ATPase activity of the cystic fibrosis transmembrane conductance regulator. *Biochemistry,* **40**:10700-6.

169. Rosenberg MF, Callaghan R, Ford RC, Higgins CF. (1997) Structure of the multidrug resistance P-glycoprotein to 2.5 nm resolution determined by electron microscopy and image analysis. *J. Biol Chem*., **272**: 10685-94.

170. Loo TW, Clarke DM. (1999a). The glycosylation and orientation in the membrane of the third cytoplasmic loop of human P-glycoprotein is affected by mutations and substrates. *Biochemistry*, **38**: 5124-9.

171. Loo TW, Clarke DM. (1999b) Identification of residues in the drug-binding domain of human P-glycoprotein. Analysis of transmembrane segment 11 by cysteine-scanning mutagenesis and inhibition by dibromobimane. *J Biol Chem*., **274**:35388-92

174. Locher KP, Lee AT, Rees DC. (2002) The *E. coli* BtuCD structure: a framework for ABC transporter architecture and mechanism. *Science,* **296**:1091-8.

173. Miller C. (1982) Open-state structure of single chloride channels from *Torpedo electroplax. Phil. Trans. Roy. Soc. London,* **299**:401-411.

174. Ludewig U, Pusch M, Jentsch TJ. (1996) Two physically distinct pores in the dimeric ClC-0 chloride channel. *Nature,* **383**:340-3.

175. Weinreich F, Jentsch TJ. (2001) Pores formed by single subunits in the mixed dimers of different ClC chloride channels. *J Biol Chem*., **276**:2347-53.

176. Dutzler R, Campbell EB, Cadene M, Chait BT, MacKinnon R. (2002) X-ray structure of a ClC chloride channel at 3.0 Å reveals the molecular basis of anion selectivity. *Nature,* **415**: 287-94.

177. Schwalbe RA, Wingo CS, Xia SL. (2002) Mutations in the putative pore-forming segment favor short-lived wild-type Kir2.1 pore conformations. *Biochemistry*, **41**:12457-66.

9. Publications of Ph.D. candidate

1. List of publication related to the thesis

Peer reviewed articles

1) Zhang Z-R, G. Cui., S. Zeltwanger, and N. A. McCarty (2004). Time-dependent interactions of Glibenclamide with CFTR: kinetically complex block of macroscopic currents. ***J. Membrane Biol***, 201(3): 139-155.

2) Zhang Z-R, G. Cui, X. Liu, B. Song, D. C. Dawson and N. A. McCarty. (2005) Determination of the functional unit of the CFTR chloride channel: One polypeptide forms one pore. ***J. Biol. Chem.*** 280(1):458-468.

3) Fuller, M. D., **Z-R Zhang,** G. Cui, and N. A. McCarty. (2005) The block of CFTR by scorpion is state dependent. ***Biophys. J.*** 89(6):3960-75.

4) Zhang Z-R, Binlin Song, and McCarty N. A. (2005) State-dependent modification of R334C by $MTSET^+$ reveals conformational change in the outer vestibule of CFTR. ***J. Biol. Chem.*** 280(51):41997-42003.

5) Thompson, C.H., D.M. Fields, P.R. Olivetti, M.D. Fuller, **Z.-R. Zhang**, J. Kubanek, and N.A. McCarty. (2005) Inhibition of ClC-2 Cl- channels by a peptide component of scorpion venom. ***J. Membrane Biol***. 208(1):65-76.

6) Cui G., **Z-R Zhang,** B. Song, and N. A. McCarty. (2007) Mutations at arginine 352 alter the pore architecture of CFTR (in press for ***J. Membrane Biol.***)

2. Other publications

Peer reviewed articles

1) Kokko KE, P. S. Matsumoto, **Z-R Zhang,** B. N. Ling, and D. C. Eaton. (1997). Prostaglandin E_2 Increases Cl^- Channel Density in the Apical Membrane of A6 Distal Nephron Cells. ***Am. J. Physiol.*** 273 (***Cell Physiol.*** 42): C548-C557.

2) Zhang Z-R, S. Zeltwanger, and N. A. McCarty (2000). Direct Comparison of NPPB and DPC as Probes for CFTR Expressed in *Xenopus* oocytes. ***J. Membrane Biol.*** 175, 35-52.

3) Zhang Z-R, S. McDonough, and N. A. McCarty (2000). Interaction between Permeation and Gating in a Putative Pore- domain Mutant in CFTR. ***Biophys. J.*** 79, 298-313.

4) McCarty N. A. and **Z-R Zhang**. (2001). Identification of a region of strong discrimination in the pore of CFTR. ***Am. J. Physiol. Lung***, 281: L852-L867.

5) Smith SS., X. Liu, **Z-R Zhang**, F. Sun, T. E. Kriewall, N. A. McCarty and D. C. Dawson. (2001). CFTR: Covalent and non covalent modification suggests a role for fixed charges in anion conduction. ***J. of General Physiol*** 118: 407-431.

6) Zhang Z-R, S. Zeltwanger, and N. A. McCarty (2002). Voltage-sensitive Gating induced by a mutation in the fifth transmembrane domain of CFTR. ***Am. J. Physiol Lung***, 282: L135-L145.

7) Liu, X. **Z-R Zhang,** M. D. Fuller, J. Billingsly, N. A. McCarty and D. C. Dawson. (2004) CFTR: A cysteine at 338 senses a positive electrostatic potential in the pore. ***Biophys. J.*** 87(6):3826-3841.

8) Zhang Z-R, S. Zeltwanger, and N. A. McCarty (2004). Steady-sate Interaction of Glibenclamide with CFTR: *Evidence for multiple sites of inhibition.* ***J. Membrane Biol***, 199(1):15-28.

9) Fuller, M. D., **Z-R Zhang,** G. Cui, and N. A. McCarty (2004). CFTR Channel Inhibition by a Peptide Toxin of Scorpion Venom. ***Am. J. Physiol*** (***Cell Physiol)***. 287(5): C1328-C1341.

10) Chien L-T, **Z.-R. Zhang**, and H. C. Hartzell. (2006) Single Cl^- channels activated by Ca^{2+} in Drosophila S2 cells are mediated by Bestrophins. ***J. of General Physiol.*** 128(3):247-59.

11) Fuller, M., C.H. Thompson, **Z.-R. Zhang**, D. McMaster, R. J. French, J Pohl, J. Kubanek, and N. A. McCarty. (2007) Inhibition of CFTR chloride channels by a novel peptide toxin . ***J. Biol. Chem.*** 282(52):37545-55

12) Bao, H., **Z.-R. Zhang**, Y-Y Liang, D. C. Eaton, and H-P Ma (2007) Ceramide mediates inhibition of the renal epithelial sodium channel by tumor necrosis factor α through protein kinase C. ***Am. J. Physiol Renal***, 293:F1178-1186.

13) Komlosi, P., **Z.-R. Zhang,** and P. D. Bell (2008) Perimacular cells- a new cellular element in the juxtaglomerular appartus (in press for ***JASN***).

<u>Invited papers (peer-reviewed):</u>

1) A book chapter: Dawson, D.C., X. Liu, **Z-R Zhang**, and N.A. McCarty. (2003). **Anion conduction properties of CFTR**. In "**The CFTR Chloride Channel**", K. Kirk and D.C. Dawson, ed. *Eurekah.com and Kluwer Academic/Plenum.* 1-34.

2) A book chapter: Cui G., M.D. Fuller, C.H. Thompson, **Z-R Zhang**, and N. A. McCarty (2007). **Recording currents from channels and transporters in macropatches.** In "Patch-Clamp Analysis: Advanced Techniques, 2nd edition", W. Walz, editor, Human Press, Inc., Totowa, NJ. 353-371.

10. Abstract

The cystic fibrosis transmembrane conductance regulator (CFTR) functions as a chloride channel and the gene defective in cystic fibrosis encodes CFTR. We performed patch-clamp analyses in oocytes expressing CFTR mutants containing cysteines engineered at putative pore-lining positions (near the predicted outer vestibule of the CFTR pore) in transmembrane domain six to determine: 1) the minimal functional unit of CFTR and 2) to detect the conformational changes in the outer vestibule of the CFTR pore associated with ATP-dependent gating events at the nucleotide binding domains (NBDs). Wild-type CFTR exhibits distinct subconductance states, which could represent currents of separate pores or different conductance states of a single pore. In comparison, cysteine engineered mutant CFTR channels altered the duration and probability of occurrence of these subconductance states without altering their relative amplitudes. Covalent modification process of single R334C-CFTR channels by SH-modifying reagent, $MTSET^+$, monitored in real-time, resulted in simultaneous modification of all three conductance levels in a single step suggesting that functional CFTR channel confers a single pore. The modification process of R334C-CFTR upon rapid exposure to $MTSET^+$ in outside-out macropatches was described best with a single exponential function suggesting that functional CFTR channel is formed as a monomer by a single CFTR polypeptide. In contrast, modification process was much slower when channels activity was much higher, such as in the presence of additional non-hydrolyzable nucleotide, or when the R334C mutation was coupled to a second mutation, K1250A, which also enhances channel activity greatly; modification was faster in R334C/K464A-CFTR channels, which exhibit very low channel activity. In single R334C-CFTR channels studied in excised patches, modification by $MTSET^+$ occurred only during channel closed states. These data together suggest that: 1) the functional CFTR channel confers a single-pore, and is formed as a monomer by a single CFTR polypeptide; 2) the chemical reactivity of the engineered cysteine in R334C-CFTR is state-dependent, providing evidence of changes in pore conformation in the outer vestibule coupled to ATP binding and hydrolysis at the NBDs.

11. Abstract in Hungarian (Összefoglalás)

A cisztás fibrózis transzmembrán konduktancia regulátor (CFTR) egy klorid csatorna, amelynek működése nem megfelelő cisztás fibrózisban szenvedő betegekben. Jelen vizsgálatainkban olyan *Xenopus* oocita CFTR mutánsokat állítottunk elő, amelyek ciszteint tartalmaznak a hatodik transzmembrán szakasz pórusképző (külső vesztibulum) régiójában, majd patch-clamp analízissel vizsgáltuk, hogy (1) mely részek szükségesek feltétlenül a CFTR működéséhez, (2) mely konformációs válozások történnek a CFTR pórusának külső vesztibulumában a nukleotid-kötő domén ATP-függő kapuzási működése során. A CFTR csatorna aktiválása érdekében ATP-t és protein kináz A-t használtunk. A vad-típusú CFTR számos részleges konduktanciájú állapotban létezhet, ezek vagy elkülönült pórusokon átfolyó áramokból, vagy egy pórus különböző konduktanciájú állapotaiból származnak. A CFTR módosításai, amelyekben cisztein helyettesít bizonyos aminosavakat, csak ezen részleges konduktanciájú állapotok kinetikáját (megjelenésük valószínűségét, illetve fennmaradási idejét) változtatják meg, de amplitúdójuk változatlan marad. Miközben az egyik ilyen mutánson (R334C-CFTR) a szulfhidril csoportokat kémiailag módosítottuk $MTSET^+$-tel, mindhárom részleges konduktanciájú állapot egyidőben megváltozott, jelezve, hogy egy pórus elegendő a működőképes CFTR csatornához. Outside-out makropatch konfigurációban módosítva a R334C-CFTR mutáns szerkezetét a mért áramok változása egy egytagú exponenciális görbével jól közelíthető volt, mutatva, hogy a működőképes CFTR csatornát egy polipeptid lánc alkotja. Farmakológiai illetve genetikai módosítások azt mutatták, hogy a CFTR aktivitása és a részleges konduktanciájú állapotok változási kinetikája fordítottan arányosak. Ugyanakkor, inside-out konfigurációban a R334-CFTR mutáns kémiai módosítása csak a zárt állapotban volt lehetséges. Összességében vizsgálataink megmutatták, hogy a működőképes CFTR csatorna egy pórusból áll, s egy polipeptid elegendő felépítéséhez. Az R334C-CFTR csatorna módosított cisztein csoportjának kémiai reakcióképessége a csatorna zárt-nyitott állapotától függ, mely azt mutatja, hogy a csatorna pórusa külső vesztibulumának konformációja függ a nukleotid-kötő doménen zajló ATP kötéstől és hidrolízistől.

12. A list of three most important articles of applicant

1) Zhang Z-R, G. Cui, X. Liu, B. Song, D. C. Dawson and N. A. McCarty. (2005) Determination of the functional unit of the CFTR chloride channel: One polypeptide forms one pore. ***J. Biol. Chem.*** 280(1):458-468.

2) Zhang Z-R, Binlin Song, and McCarty N. A. (2005) State-dependent modification of R334C by $MTSET^+$ reveals conformational change in the outer vestibule of CFTR. ***J. Biol. Chem.*** 280(51):41997-42003.

3) Zhang Z-R, S. Zeltwanger, and N. A. McCarty (2004). Steady-sate Interaction of Glibenclamide with CFTR: *Evidence for multiple sites of inhibition.* ***J. Membrane Biol***, 199(1):15-28.